Bond-order potentials: derivation and parameterization for refractory elements

2015 Modelling Simul. Mater. Sci. Eng. 23 074004

(http://iopscience.iop.org/0965-0393/23/7/074004)

IOP Publishing Modelling and Simulation in Materials Science and Engineering

Modelling Simul. Mater. Sci. Eng. **23** (2015) 074004 (36pp) doi:10.1088/0965-0393/23/7/074004

Bond-order potentials: derivation and parameterization for refractory elements

Ralf Drautz[1], Thomas Hammerschmidt[1], Miroslav Čák[1] and D G Pettifor[2]

[1] ICAMS, Ruhr-Universität Bochum, 44780 Bochum, Germany
[2] Department of Materials, University of Oxford, Parks Road, Oxford, OX1 3PH, UK

E-mail: ralf.drautz@rub.de

Received 30 November 2014, revised 16 March 2015
Accepted for publication 23 March 2015
Published 18 September 2015

Abstract

The bond-order potentials are derived from density functional theory by a systematic coarse graining of the electronic structure. Within their functional form the bond-order potentials comprise covalent bond formation, charge transfer and magnetism. We review the derivation of the bond-order potentials from density functional theory and discuss their application to the simulation of refractory transition metals. We show that the derived functional form of the bond-order potentials ensures the transferability of the potentials to atomic environments that have not been taken into account in the parameterization.

Keywords: bond-order potentials, tight-binding approximation, density functional theory, atomistic simulation

(Some figures may appear in colour only in the online journal)

1. Introduction

The quality of atomistic simulations depends critically on the description of the interatomic interaction. The representation of the interatomic interaction must reproduce the bond chemistry of the system at hand for reliable simulations. A good description of the interatomic interaction is often provided by quantum mechanical methods such as density functional theory (DFT) or more accurate quantum chemical methods. Unfortunately this is of little help for simulations in which more than a few hundred atoms or more than a few thousand force evaluations are required, as then the computer time required for the DFT simulations becomes prohibitively expensive. In many simulations therefore empirical potentials are used that are orders of magnitude faster than DFT and enable the simulation of many thousands or millions of atoms.

The functional form of empirical potentials such as, for example, the embedded atom method potentials [1, 2] or the Tersoff potential [3] and their modern extensions is not derived but motivated by heuristic considerations and often adapted for the simulation of new materials. The parameters in the empirical potentials are fitted to reproduce experimental data or DFT calculations. Because empirical potentials are limited in their functional form, they are typically only reliable for the simulation of atomic configurations that are close to configurations used in their parameterization.

To lift the inherent limitations of empirical potentials, researchers have recently abandoned using any functional form. In the GAP [4], SNAP [5] or neural network potentials [6] a formal mathematical expansion of the continuous space of atomic configurations is carried out and then parameterized using many DFT calculations until, based on statistical analysis, the expansion may be used to predict the energy of atomic configurations not used in the fit with some confidence.

The Bond-Order Potentials (BOPs) are different from both, the empirical potentials on the one hand and the formal expansions on the other hand. The BOPs are *derived* by a systematic coarse graining of DFT. In this way the functional form of the BOPs comprises the bond chemistry of the system at hand and is therefore transferable to different atomic configurations, so that the BOPs are not limited by their functional form in the way empirical potentials are. At the same time, because of the derived functional form of the BOPs, the number of parameters required for their parameterization is relatively small so that their fitting does not require large reference data sets, as they are required for a formal mathematical expansion. In short, by deriving the functional form of the BOPs we expect that they contain more physics. This implies that we expect a reliable prediction for atomic configurations that were not taken into account in the fit, or in other words, a robust transferability.

The transferability of the BOPs away from reference atomic configurations will be demonstrated in this paper. We will focus on refractory transition metals and show how a straightforward fitting strategy together with the derived functional form of the BOPs enables a good prediction of atomic configurations that were not used in the fit.

Before discussing the fitting strategy we will outline the derivation of the BOPs from DFT. In a first step of coarse graining, DFT is simplified to the Tight-Binding (TB) approximation. This comprises a formal expansion of the DFT functional with respect to charge fluctuations and the representation of the DFT wavefunction in an optimized atomic-like basis. The resulting energy is then represented in the TB bond model [7, 8], which provides a transparent and intuitive framework for modelling the interatomic interaction, including covalent bond formation, charge transfer and magnetism. The TB approximation has been discussed in detail in the literature [9–13] and we limit our discussion to the minimum required for a coherent derivation of the TB bond model. In a second step of coarse graining a general, local approximation to the solution of the TB bond model is constructed. This leads directly to the BOPs. We briefly discuss the BOP expansion, their extension to magnetism and the evaluation of atomic forces and magnetic torques using the BOPs.

The paper is structured as follows. In section 2 we summarize the essential basics of the second-order DFT expansion. The general second-order expansion is then discussed for the TB approximation in section 3. In section 4 the TB bond model is introduced and the different contributions to the energy in the TB bond model are derived. The bond-order potential expansion is then summarized in section 5. In section 6 the parameterization of the BOPs for refractory elements is presented and examples of the application of the BOPs are given.

2. Expansion of the density functional

2.1. DFT basics

In DFT the energy is expressed as a functional of the charge density ρ, or the spin-charge density for magnetic systems,

$$U = U[\rho]\,. \tag{1}$$

Magnetism will not be discussed here, but the extension from non-magnetic to magnetic systems is not very complicated [14, 15] and has been discussed in detail in [8]. In fact, a large part of this section corresponds to a simplified presentation of [8] excluding magnetism.

The ground state energy U_0 of the density functional may be determined from the variational optimization of the energy U with respect to the charge density ρ,

$$U_0 \leqslant U[\rho]\,. \tag{2}$$

A key feature of standard DFT is the representation of the charge density $\rho\,(\boldsymbol{r})$ from single-electron wavefunctions

$$\rho(\boldsymbol{r}) = \sum_n f_n \psi_n(\boldsymbol{r})\psi_n^*(\boldsymbol{r})\,. \tag{3}$$

The wavefunctions are eigenstates of the Kohn–Sham DFT Hamiltonian

$$\hat{H}\psi_n(\boldsymbol{r}) = \epsilon_n\psi_n(\boldsymbol{r})\,, \tag{4}$$

and the occupation number f_n is two for a fully occupied eigenstate with eigenvalue ϵ_n below the Fermi energy and zero for an empty state above the Fermi energy. When the wavefunctions are expanded in a basis

$$\psi_n = \sum_i c_i^{(n)}\varphi_i(\boldsymbol{r})\,, \tag{5}$$

the charge density is represented as

$$\rho(\boldsymbol{r}) = \sum_{ij} n_{ij}\varphi_i^*(\boldsymbol{r})\varphi_j(\boldsymbol{r})\,, \tag{6}$$

with the elements of the density matrix

$$n_{ij} = \sum_n f_n c_i^{*(n)} c_j^{(n)}\,. \tag{7}$$

The density matrix $\boldsymbol{n}$ is also referred to as the bond order and a key quantity in the bond-order potentials. This will be discussed in some detail in section 3.2. As we will also see later, in TB the basis functions are usually taken as atomic-like functions that are non-orthogonal

$$S_{ij} = \langle\varphi_i|\varphi_j\rangle = \int \varphi_i^*(\boldsymbol{r})\varphi_j(\boldsymbol{r})\,\mathrm{d}\boldsymbol{r}\,, \tag{8}$$

with the overlap matrix $\boldsymbol{S}$. The norm of the wavefunctions is written as

$$N_n = \langle\psi_n|\psi_n\rangle = c_i^{*(n)} c_j^{(n)} S_{ij} = 1\,. \tag{9}$$

From this the total number of electrons is obtained as

$$N = \sum_n f_n N_n = \sum_{ij} n_{ij} S_{ji} \,, \tag{10}$$

and a possible definition of the number of electrons in orbital i may be written as

$$N_i = \sum_j n_{ij} S_{ji} \,. \tag{11}$$

This is the Mulliken charge. Things are easier in an orthonormal basis, where

$$N_i = n_{ii} \,, \tag{12}$$

so that N_i is only associated with orbital i.

A representation in an orthogonal basis can be obtained by defining new basis functions as

$$|\phi_i\rangle = |\varphi_j\rangle S_{ji}^{-1/2} \,, \tag{13}$$

where we used the Einstein summation convention. Therefore

$$\langle\phi_i| = S_{ij}^{-1/2} \langle\varphi_j| \,, \tag{14}$$

so that

$$\langle\phi_i|\phi_j\rangle = S_{ik}^{-1/2} S_{kl}\, S_{lj}^{-1/2} = \delta_{ij} \,. \tag{15}$$

This is called a Löwdin transformation [16]. Matrix elements of an operator $\hat{A}$ in the new basis are written as

$$\tilde{A}_{ij} = \langle\phi_i|\hat{A}|\phi_j\rangle = S_{ik}^{-1/2} \langle\varphi_k|\hat{A}|\varphi_l\rangle S_{lj}^{-1/2} = S_{ik}^{-1/2} A_{kl}\, S_{lj}^{-1/2} \,. \tag{16}$$

Here it is useful to note that the diagonal elements of the overlap matrix are equal to one and it is customary to separate the diagonal part from the rest

$$S_{ij} = \delta_{ij} + O_{ij} \,, \tag{17}$$

where $O_{ij} = S_{ij}$ for $i \neq j$ and zero otherwise. Next we separate $\boldsymbol{S}^{-1/2}$ in a similar way,

$$S_{ij}^{-1/2} = \delta_{ij} - \frac{1}{2} \mathfrak{S}_{ij} \,. \tag{18}$$

This choice of $\boldsymbol{\mathfrak{S}}$ is motivated from the fact that it is given to first order by $\boldsymbol{O}$,

$$\mathfrak{S}_{ij} = O_{ij} + \mathcal{O}(2) \,, \tag{19}$$

and in some cases it may be assumed that $|O_{ij}| \ll 1$, so that a first order expansion is sufficient. Equation (16) is now written as

$$\tilde{A}_{ij} = A_{ij} - \frac{1}{2}(A_{ik}\mathfrak{S}_{kj} + \mathfrak{S}_{ik}A_{kj}) \; + \frac{1}{4}\mathfrak{S}_{ik}A_{kl}\mathfrak{S}_{lj} \,. \tag{20}$$

2.2. Contributions to the DFT energy

Following the expansion of the charge density in a basis, equation (6), the DFT energy may be written as an ordinary function of the density matrix $\boldsymbol{n}$,

$$U = U(\boldsymbol{n}) = T_\mathrm{S} + U_\mathrm{H} + U_\mathrm{XC} + U_\mathrm{ext} + U_\mathrm{nuc}\,, \tag{21}$$

that is easily categorized in first, second and higher-order contributions in terms of the density matrix. The interaction of the bare ionic cores U_nuc is independent of the charge density. The first-order terms are given by the kinetic energy of the non-interacting electrons that is expressed in single-electron wavefunctions as

$$T_\mathrm{S} = \sum_n f_n \langle \psi_n | \hat{T} | \psi_n \rangle = \boldsymbol{T}\boldsymbol{n}\,, \tag{22}$$

where also here and in the following unless noted otherwise the Einstein summation is used so that the sum over all pairwise indices is taken. To simplify the notation further we often leave away the indices completely, for example, the trace of the product of the matrices $\boldsymbol{T}$ and $\boldsymbol{n}$ is written as

$$\boldsymbol{T}\boldsymbol{n} = \sum_{ij} T_{ij} n_{ji}\,. \tag{23}$$

The matrix elements of the kinetic energy $\boldsymbol{T}$ are given by

$$T_{ij} = \langle \varphi_i | \hat{T} | \varphi_j \rangle\,. \tag{24}$$

The external energy U_ext contains the coupling of the electrons to an external potential. In DFT it is common to view the interaction of the electrons with the ionic cores as part of the external potential. The external energy is a first-order term with respect to the expansion of the energy in terms of the density matrix,

$$U_\mathrm{ext} = \int V^\mathrm{ext}(\boldsymbol{r})\rho(\boldsymbol{r})\,\mathrm{d}\boldsymbol{r} = \boldsymbol{V}^\mathrm{ext}\boldsymbol{n}\,, \tag{25}$$

with the matrix elements of the external potential

$$V^\mathrm{ext}_{ij} = \int \varphi_i^*(\boldsymbol{r}) V^\mathrm{ext}(\boldsymbol{r}) \varphi_j(\boldsymbol{r})\,\mathrm{d}\boldsymbol{r}\,. \tag{26}$$

The Hartree energy U_H is of second order in $\boldsymbol{n}$ or the density ρ,

$$U_\mathrm{H} = \frac{1}{2}\int \frac{\rho(\boldsymbol{r})\rho(\boldsymbol{r}')}{|\boldsymbol{r}-\boldsymbol{r}'|}\mathrm{d}\boldsymbol{r}\mathrm{d}\boldsymbol{r}' = \sum_{ijkl}\frac{1}{2}J^\mathrm{H}_{ijkl} n_{ij} n_{kl} = \frac{1}{2}\boldsymbol{J}^\mathrm{H}\boldsymbol{n}\boldsymbol{n}\,, \tag{27}$$

with

$$J^\mathrm{H}_{ijkl} = \frac{1}{2}\int \frac{\varphi_i^*(\boldsymbol{r})\varphi_j(\boldsymbol{r})\varphi_k^*(\boldsymbol{r}')\varphi_l(\boldsymbol{r}')}{|\boldsymbol{r}-\boldsymbol{r}'|}\mathrm{d}\boldsymbol{r}\mathrm{d}\boldsymbol{r}'\,. \tag{28}$$

The exchange-correlation energy U_XC is usually parameterized as a non-linear functional of ρ and therefore the only contribution to the DFT energy that contains terms beyond second order. Here we just write a formal series expansion[3] as

$$U_\mathrm{XC} = \boldsymbol{V}^\mathrm{XC}\boldsymbol{n} + \frac{1}{2}\boldsymbol{J}^\mathrm{XC}\boldsymbol{n}\boldsymbol{n} + \frac{1}{6}\boldsymbol{K}^\mathrm{XC}\boldsymbol{n}\boldsymbol{n}\boldsymbol{n} + \cdots\,. \tag{29}$$

As the exchange-correlation energy contains the corrections due to many-electron interactions, it is relatively short ranged. For example, while $\boldsymbol{J}^\mathrm{H}$ decays like $1/r$ for large separations

[3] Note that a series expansion formally is not always possible, for example, an expansion of $\rho^{4/3}$ at $\rho_0 = 0$. This formal problem will, however, be avoided by an expansion at $\rho_0 \neq 0$ that we will make use of in section 2.5.

between the orbitals, we expect that the term $\boldsymbol{J}^{\mathrm{XC}}$ is limited to distances of the order of the interatomic separation. This also holds in spin-density functional theory, where magnetism enters the DFT energy only through the exchange correlation energy and gives rise to relatively short-ranged terms. The lowest contribution of magnetism is of second order, $-\frac{1}{4}\boldsymbol{I}^{\mathrm{XC}}\boldsymbol{mm}$, where $\boldsymbol{m}$ are the matrix elements of the magnetization density and $\boldsymbol{I}^{\mathrm{XC}}$ at $r = 0$ the Stoner exchange integral.

By grouping

$$\boldsymbol{V} = \boldsymbol{V}^{\mathrm{ext}} + \boldsymbol{V}^{\mathrm{XC}}\,, \quad \boldsymbol{J} = \boldsymbol{J}^{\mathrm{H}} + \boldsymbol{J}^{\mathrm{XC}}\,, \quad \boldsymbol{K} = \boldsymbol{K}^{\mathrm{XC}}\,, \tag{30}$$

the DFT energy is now written in the form of a series expansion in the density matrix

$$U = U_{\mathrm{nuc}} + (\boldsymbol{T} + \boldsymbol{V})\boldsymbol{n} + \frac{1}{2}\boldsymbol{Jnn} + \frac{1}{6}\boldsymbol{Knnn} + \cdots\,. \tag{31}$$

2.3. Hamiltonian and band energy

As we have seen in equation (6), for a given basis the charge density is fully specified by the density matrix. Therefore the variational derivative that needs to be evaluated for optimizing the DFT energy with respect to the charge density $\frac{\delta U}{\delta \rho}$ becomes an ordinary derivative with respect to the matrix elements of the density matrix, $\frac{\partial U}{\partial \boldsymbol{n}}$. This derivative may be taken as the definition of the effective one-electron Hamiltonian matrix

$$\boldsymbol{H} = \frac{\partial U}{\partial \boldsymbol{n}} = \boldsymbol{T} + \boldsymbol{V} + \boldsymbol{Jn} + \frac{1}{2}\boldsymbol{Knn} + \cdots\,. \tag{32}$$

For the moment we will just accept this definition of the effective one-electron Hamiltonian matrix and will discuss its implications later. The DFT energy is then usually represented as the band energy $U_{\mathrm{band}} = \boldsymbol{Hn}$ and the so-called double-counting contribution U_{dc},

$$\begin{aligned} U &= U_{\mathrm{nuc}} + U_{\mathrm{band}} + U_{\mathrm{dc}} \\ &= U_{\mathrm{nuc}} + \boldsymbol{Hn} - \frac{1}{2}\boldsymbol{Jnn} - \frac{1}{3}\boldsymbol{Knnn} - \cdots\,. \end{aligned} \tag{33}$$

The second-order term is contained in $\boldsymbol{Hn}$ twice and therefore has to be subtracted from the energy in the double-counting contribution. For higher-order contributions the pre-factor in the correction is not 1/2 but $(k-1)/k!$, where k is the order of the contribution in the expansion.

2.4. Energy minimization and Kohn–Sham equations

In a given basis the wavefunctions are determined by the expansion coefficients $c_j^{(n)}$. At the minimum of the energy with respect to the orthogonal one-electron wavefunctions, derivatives with respect to the expansion coefficients fulfill

$$\frac{\partial}{\partial c_j^{*(n)}}\left(U - \sum_n \epsilon_n N_n\right) = 0\,, \tag{34}$$

where $N_n = \sum_i c_i^{*(n)} c_j^{(n)} S_{ij}$ from equation (9) and where the Lagrange multipliers ϵ_n ensure that the one-electron wavefunctions are normalized, $N_n = 1$.

From equation (32) and by making use of the chain rule, we immediately recover the usual Kohn–Sham equations equation (4) in matrix form (the secular equation),

$$\sum_i \Big(H_{ji} - \epsilon_n S_{ji} \Big) c_i^{(n)} = 0 \,, \tag{35}$$

or in matrix notation

$$(\boldsymbol{H} - \epsilon_n \boldsymbol{S}) \boldsymbol{c}^{(n)} = 0 \,. \tag{36}$$

As $\boldsymbol{H}$ is a function of $\boldsymbol{n}$, the Kohn–Sham equations are typically solved iteratively:

(a) estimate or guess $\boldsymbol{n}^{(\mathrm{in})}$,
(b) compute $\boldsymbol{H}^{(\mathrm{in})} = \boldsymbol{H}(\boldsymbol{n}^{(\mathrm{in})})$,
(c) solve equation (35) and compute $\boldsymbol{n}^{(\mathrm{out})} = \sum_n f_n \boldsymbol{c}^{*(n)} \boldsymbol{c}^{(n)}$,
(d) modify $\boldsymbol{n}^{(\mathrm{in})}$, return to (a) and iterate until $\boldsymbol{n}^{(\mathrm{in})} = \boldsymbol{n}^{(\mathrm{out})}$.

If the condition $\boldsymbol{n}^{(\mathrm{in})} = \boldsymbol{n}^{(\mathrm{out})}$ is fulfilled within a given numerical accuracy, one has found an extremum of the energy. As then the input and output charge density are identical, this is often referred to as a self-consistent solution. Clearly, the energy during the iteration is always larger or equal to the ground state energy, $U\,(\boldsymbol{n}^{(\mathrm{in})}) \geqslant U_0$ and is explicitly given by

$$\begin{aligned} U(\boldsymbol{n}^{(\mathrm{in})}) &= U_{\mathrm{nuc}} + (\boldsymbol{T} + \boldsymbol{V}) \boldsymbol{n}^{(\mathrm{out})} + \frac{1}{2} \boldsymbol{J} \boldsymbol{n}^{(\mathrm{out})} \boldsymbol{n}^{(\mathrm{out})} + \frac{1}{6} \boldsymbol{K} \boldsymbol{n}^{(\mathrm{out})} \boldsymbol{n}^{(\mathrm{out})} \boldsymbol{n}^{(\mathrm{out})} + \cdots \,, \\ &= U_{\mathrm{nuc}} + \boldsymbol{H}^{(\mathrm{in})} \boldsymbol{n}^{(\mathrm{out})} + \frac{1}{2} \boldsymbol{J} (\boldsymbol{n}^{(\mathrm{out})} - 2\boldsymbol{n}^{(\mathrm{in})})\, \boldsymbol{n}^{(\mathrm{out})} \\ &\quad + \frac{1}{6} \boldsymbol{K} (\boldsymbol{n}^{(\mathrm{out})} \boldsymbol{n}^{(\mathrm{out})} - 3\boldsymbol{n}^{(\mathrm{in})} \boldsymbol{n}^{(\mathrm{in})})\, \boldsymbol{n}^{(\mathrm{out})} + \cdots \,. \end{aligned} \tag{37}$$

This is an unfortunate representation of the energy as the (in) and (out) quantities are mixed, which also makes it difficult to achieve an understanding or interpretation.

2.5. Expansion with respect to a reference density

By re-expanding the series expansion equation (31) about a reference charge density $\rho^{(0)}$ or equivalently a reference density matrix $\boldsymbol{n}^{(0)}$ such that

$$\boldsymbol{n} = \boldsymbol{n}^{(0)} + \delta \boldsymbol{n} \,, \tag{38}$$

the problem of mixing (in) and (out) quantities in the expression for the energy is resolved. From equation (31) one obtains

$$U = U^{(0)} + \boldsymbol{H}^{(0)} \delta \boldsymbol{n} + \frac{1}{2} \boldsymbol{J} \delta \boldsymbol{n}\, \delta \boldsymbol{n} + \frac{1}{6} \boldsymbol{K} (3 \boldsymbol{n}^{(0)} \delta \boldsymbol{n}\, \delta \boldsymbol{n} + \delta \boldsymbol{n}\, \delta \boldsymbol{n}\, \delta \boldsymbol{n}) + \cdots \,. \tag{39}$$

Not surprisingly second-order terms in $\delta \boldsymbol{n}$ contain contributions from third-order and higher-order contributions in $\boldsymbol{n}$. The energy $U^{(0)}$ at the reference density is given by

$$U^{(0)} = U_{\mathrm{nuc}} + \boldsymbol{H}^{(0)} \boldsymbol{n}^{(0)} - \frac{1}{2} \boldsymbol{J} \boldsymbol{n}^{(0)} \boldsymbol{n}^{(0)} - \frac{1}{3} \boldsymbol{K} \boldsymbol{n}^{(0)} \boldsymbol{n}^{(0)} \boldsymbol{n}^{(0)} - \cdots \,, \tag{40}$$

such that an expression for the energy may be written as

$$U = U_{\mathrm{nuc}} + \boldsymbol{H}^{(0)}\boldsymbol{n} + \frac{1}{2}\boldsymbol{J}'\delta\boldsymbol{n}\,\delta\boldsymbol{n} + \frac{1}{6}\boldsymbol{K}'\delta\boldsymbol{n}\,\delta\boldsymbol{n}\,\delta\boldsymbol{n} - \frac{1}{2}\boldsymbol{J}\boldsymbol{n}^{(0)}\boldsymbol{n}^{(0)} - \frac{1}{3}\boldsymbol{K}\boldsymbol{n}^{(0)}\boldsymbol{n}^{(0)}\boldsymbol{n}^{(0)}\cdots\,, \tag{41}$$

and where $\boldsymbol{J}'$ and $\boldsymbol{K}'$ refer to the second and third-order expansion coefficients about $\boldsymbol{n}^{(0)}$. The Hamiltonian is obtained as

$$\boldsymbol{H} = \boldsymbol{H}^{(0)} + \boldsymbol{J}'\delta\boldsymbol{n} + \frac{1}{2}\boldsymbol{K}'\delta\boldsymbol{n}\delta\boldsymbol{n} + \cdots\,. \tag{42}$$

The iterative solution now proceeds in a similiar way as before,

(a) estimate or guess $\delta\boldsymbol{n}^{(\mathrm{in})}$,
(b) compute $\boldsymbol{H}^{(\mathrm{in})}$,
(c) solve equation (35) and compute $\boldsymbol{n}^{(\mathrm{out})} = \sum_n f_n \boldsymbol{c}^{*(n)}\boldsymbol{c}^{(n)}$,
(d) modify $\delta\boldsymbol{n}^{(\mathrm{in})}$, return to (a) and iterate until $\boldsymbol{n}^{(\mathrm{in})} = \boldsymbol{n}^{(\mathrm{out})}$.

During the iteration the Hamiltonian and the energy are given by

$$\boldsymbol{H} = \boldsymbol{H}^{(0)} + \boldsymbol{J}'\delta\boldsymbol{n}^{(\mathrm{in})} + \frac{1}{2}\boldsymbol{K}'\delta\boldsymbol{n}^{(\mathrm{in})}\delta\boldsymbol{n}^{(\mathrm{in})} + \cdots \tag{43}$$

and

$$\begin{aligned} U = U_{\mathrm{nuc}} &+ \boldsymbol{H}^{(0)}\boldsymbol{n}^{(\mathrm{out})} + \frac{1}{2}\boldsymbol{J}'\delta\boldsymbol{n}^{(\mathrm{out})}\delta\boldsymbol{n}^{(\mathrm{out})} + \frac{1}{6}\boldsymbol{K}'\delta\boldsymbol{n}^{(\mathrm{out})}\delta\boldsymbol{n}^{(\mathrm{out})}\delta\boldsymbol{n}^{(\mathrm{out})} \\ &- \frac{1}{2}\boldsymbol{J}\boldsymbol{n}^{(0)}\boldsymbol{n}^{(0)} - \frac{1}{3}\boldsymbol{K}\boldsymbol{n}^{(0)}\boldsymbol{n}^{(0)}\boldsymbol{n}^{(0)}\cdots\,. \end{aligned} \tag{44}$$

As the Hamiltonian and the energy only depend on (in) and (out) quantities, respectively and not a mixture of the two, it is now straightfoward to work with the Hamiltonian or the energy even if the charge density is not self-consistent. Therefore we will also drop (in) and (out) in the following sections.

2.6. Variation with respect to the Hamiltonian

By writing the density matrix $\boldsymbol{n}$ in the form of the difference $\delta\boldsymbol{n}$ to a reference density matrix $\boldsymbol{n}^{(0)}$, the energy could be written as a function of $\boldsymbol{n}^{(\mathrm{out})}$, equation (44). The (out) density matrix depends only on $\boldsymbol{H}^{(\mathrm{in})}$, while $\boldsymbol{H}^{(\mathrm{in})}$ is a function of $\boldsymbol{n}^{(\mathrm{in})}$. This relation is expressed formally as

$$U = U(\boldsymbol{n}^{(\mathrm{out})}(\boldsymbol{H}^{(\mathrm{in})}(\boldsymbol{n}^{(\mathrm{in})})))\,. \tag{45}$$

The input density matrix $\boldsymbol{n}^{(\mathrm{in})}$ is guessed to provide an estimate for $\boldsymbol{H}^{(\mathrm{in})}$, but this is only one way to generate a suitable Hamiltonian $\boldsymbol{H}^{(\mathrm{in})}$. If one can find a way to estimate $\boldsymbol{H}^{(\mathrm{in})}$ directly without computing it from $\boldsymbol{n}^{(\mathrm{in})}$, then the energy may be viewed as a function of $\boldsymbol{H}^{(\mathrm{in})}$,

$$U = U(\boldsymbol{n}^{(\mathrm{out})}(\boldsymbol{H}^{(\mathrm{in})}))\,. \tag{46}$$

The optimization of the energy may then be achieved by direct minimization

$$\frac{\partial U}{\partial \boldsymbol{H}^{(\mathrm{in})}} = 0\,. \tag{47}$$

This property is exploited for the bond-order potentials. In the BOPs the self-consistent iteration described in section 2.5 cannot be used as the eigenspectrum of the Hamiltonian is not exactly calculated but approximated. In this case the self-consistent solution $\boldsymbol{n}^{(\mathrm{out})} = \boldsymbol{n}^{(\mathrm{in})}$ does not correspond to an extremum of the energy.

3. Bond formation in the tight-binding approximation

3.1. The TB approximation

In the previous section a formal framework within DFT was established. This framework forms the basis for the TB approximation where particular choices for the basis functions and the reference charge density for the expansion are made. We summarize these choices and approximations in the following.

3.1.1. Second-order expansion. In the TB approximation the expansion of the energy equation (41) is typically (but not always) terminated after second order, which implies that the Hamiltonian equation (42) is a linear function of the density matrix. As argued before, this should be a good approximation to DFT as only the exchange-correlation energy includes contributions that are of higher than third order and these contributions are partly taken into account in equation (41).

3.1.2. Overlapping atomic-like charge density. The reference charge density $\boldsymbol{n}^{(0)}$ and the reference Hamiltonian $\boldsymbol{H}^{(0)}$ are obtained by placing charge neutral, non-magnetic atoms on positions for which the calculation will be carried out and by then overlapping the charge densities of the atoms.

3.1.3. Local basis. The one-electron eigenstates are expanded as a linear combination of atomic orbital-type (LCAO) basis functions. Orbital $|i\alpha\rangle$ is located on atom i and has an angular momentum characterized by l, m. The basis functions are written as

$$\varphi_{i\alpha}(\boldsymbol{r}) = R_{nl}(|\boldsymbol{r} - \boldsymbol{r}_i|)Y_{lm}(\theta, \phi)\,, \tag{48}$$

with $\alpha = n, l, m$ and where the radial function R_{nl} depends only on the distance to the position $\boldsymbol{r}_i$ of atom i and Y_{lm} is a spherical harmonic or a real linear combination of spherical harmonics that form cubic harmonics. In the literature one also finds $|I\mu\rangle$ or $|Inlm\rangle$, etc which is essentially the same notation. When two atoms come close, their basis functions will overlap and there is in general no reason why the overlap integral equation (8) should vanish. Thus the local basis in a TB approximation is intrinsically non-orthogonal.

3.1.4. Minimal basis. Different from a typical LCAO basis that is used in DFT, where for the same angular momentum character several basis functions with different radial functions are employed, in TB one uses only one orbital for each radial function and only includes orbitals that are dictated by the chemistry of the problem at hand. For example, for carbon or silicon four orbitals are used, one s orbital and three p orbitals.

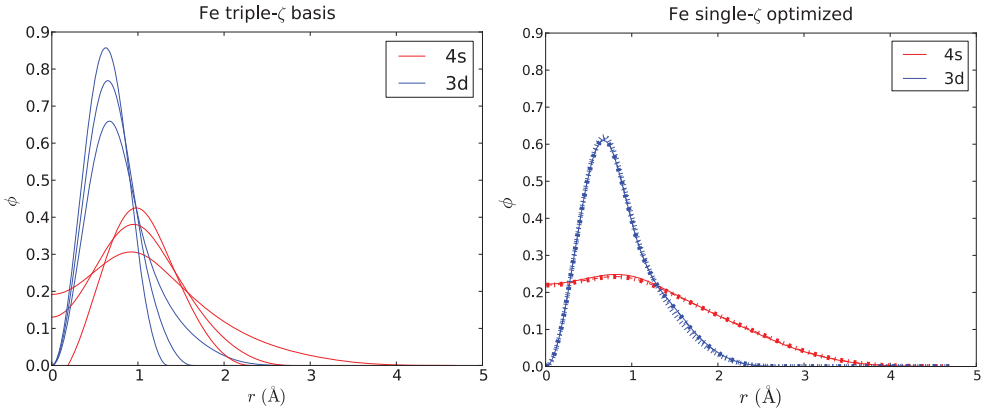

Figure 1. A single s and a single d radial function for Fe (right) are obtained from multiple s and d radial functions (left). After [17].

The radial function of the TB-orbitals must be modified away from the radial function of a free atom in order that a good representation of the reference DFT eigenstates may be achieved. Automated procedures for this optimization have been developed [17, 18]. Figure 1 shows an application for a non-orthogonal *sd*-valent TB model of Fe.

The local atomic-like basis together with the choice of the reference charge density $\boldsymbol{n}^{(0)}$ as overlapping atomic charges allows for a chemically intuitive and physically transparent analysis of bond formation in the TB approximation. In the following we will briefly discuss the important contributions to bond formation in TB.

3.2. Bond order and density matrix

The atomic-like minimal basis that is used in TB allows for a chemically intuitive interpretation of bond formation. The effectiveness of bond formation is thereby characterised by the bond order. The bond order is the same as the density matrix, a factor of two relating them in non-magnetic systems where every eigenstate may be occupied by two electrons of opposite spin

$$\Theta_{i\alpha j\beta} = 2\, n_{i\alpha j\beta}\,. \tag{49}$$

To see how the density matrix quantifies the strength of a bond, i.e. its bond order, we transform the orbitals $|i\alpha\rangle$ and $|j\beta\rangle$ of an orthogonal TB model in a new basis of bonding and anti-bonding dimer-like states

$$|+\rangle = \frac{1}{\sqrt{2}}(|i\alpha\rangle + |j\beta\rangle) \quad \text{bonding state}\,, \tag{50}$$

$$|-\rangle = \frac{1}{\sqrt{2}}(|i\alpha\rangle - |j\beta\rangle) \quad \text{anti-bonding state}\,. \tag{51}$$

Then

$$\Theta_{i\alpha j\beta} = 2\langle i\alpha|\hat{n}|j\beta\rangle = \frac{1}{2}(N_+ - N_-)\,, \tag{52}$$

with $N_+ = 2\langle +|\hat{n}|+\rangle$ and $N_- = 2\langle -|\hat{n}|-\rangle$. Therefore the density matrix is just half the difference of the number of electrons in bonding and anti-bonding states. The number of electrons in the bond is given by $N_{i\alpha i\alpha} + N_{j\beta j\beta} = N_+ + N_-$. Thus, if we assume a non-magnetic calculation and take into account spin degeneracy, then $0 \leqslant N_{i\alpha i\alpha} \leqslant 2$ and the same for $N_{j\beta j\beta}$, so that we can immediately put limits on the bond order

$$|\Theta_{i\alpha j\beta}| \leqslant N_{i\alpha j\beta}\,, \tag{53}$$

$$|\Theta_{i\alpha j\beta}| \leqslant 2 - N_{i\alpha j\beta}\,, \tag{54}$$

with $N_{i\alpha j\beta} = \frac{1}{2}(N_{i\alpha i\alpha} + N_{j\beta j\beta})$. Figure 2 illustrates the behaviour of the density matrix as a function of band filling. It shows the formation of σ and π bonds in a *sp*-valent orthogonal TB model Hamiltonian that approximately corresponds to silicon but does not include any *sp*-splitting ($E_p - E_s$) that is responsible for the positive promotion energy of *s* to *p* electrons. If the number of valence electrons is increased from 0 to 8, the band-filling fraction runs from 0 to 1. The numbers in the plot correspond to the coordination of the structure: 1-dimer, 2-linear chain, 2′-helical chain, 3-puckered graphene, 3′-graphene, 4-diamond, 6-simple cubic, 8a and 8b axial and basal bonds respectively in simple hexagonal, 12-face centred cubic. The curves in the right-hand panel of figure 2 were calculated using the analytic bond-based BOPs [19, 20] together with an extrapolation to arbitrary band filling [21].

As can be seen from the upper left-hand panel of figure 2, all the electrons in the σ-bond are first filled into bonding states for all coordinations up to and including 4. When all bonding states are full, the anti-bonding states have to be populated and the bond order decreases from a band-filling fraction of 1/2. For higher coordinated structures, the bonding states are only partly filled and the bond order never achieves its maximum possible value. This corresponds to the formation of unsaturated bonds that also prevail in close-packed transition metals. The π-bonds are more sensitive to coordination than the σ bond, as can be seen in the lower two left-hand panels. Coordinations of 2 or 3 diminish the bond order and for coordinations of 4 or more the bond order is small. This means that π bond formation is limited to very open structures, such as graphene or molecules, whereas in the diamond lattice, for example, π bonds are essentially not formed. This explains why the empirical Tersoff potential [3] could give a sensible description of the bond formation in Si although not taking into account π bond formation [22].

3.3. Parameterization of matrix elements in the TB approximation

The energy equation (41) and the Hamiltonian equation (42) may be computed when all matrix elements $\boldsymbol{J}'$, $\boldsymbol{K}'$, etc are known. In a minimal basis DFT calculation, often the computation of the matrix elements is the most time consuming part. It is a key approximation in TB that the matrix elements are not evaluated explicitly, but parameterized with analytical or tabulated functions. This makes TB calculations much faster than minimal-basis DFT, but requires great care and extensive testing of the parameterization for a robust and transferable TB model.

3.3.1. The first-order contribution: parameterization of the Hamiltonian matrix. The Hamiltonian matrix elements $\boldsymbol{H}^{(0)}$ are often parameterized using the Slater–Koster or two-centre approximation [23], where the matrix elements $\langle i\alpha|\hat{H}|j\beta\rangle$ are assumed to depend only on the position of atoms i and j and the orbitals α and β. If the bond is rotated in the z-direction, most of the matrix elements will vanish because of the assumed cylindrical symmetry. Of the matrix

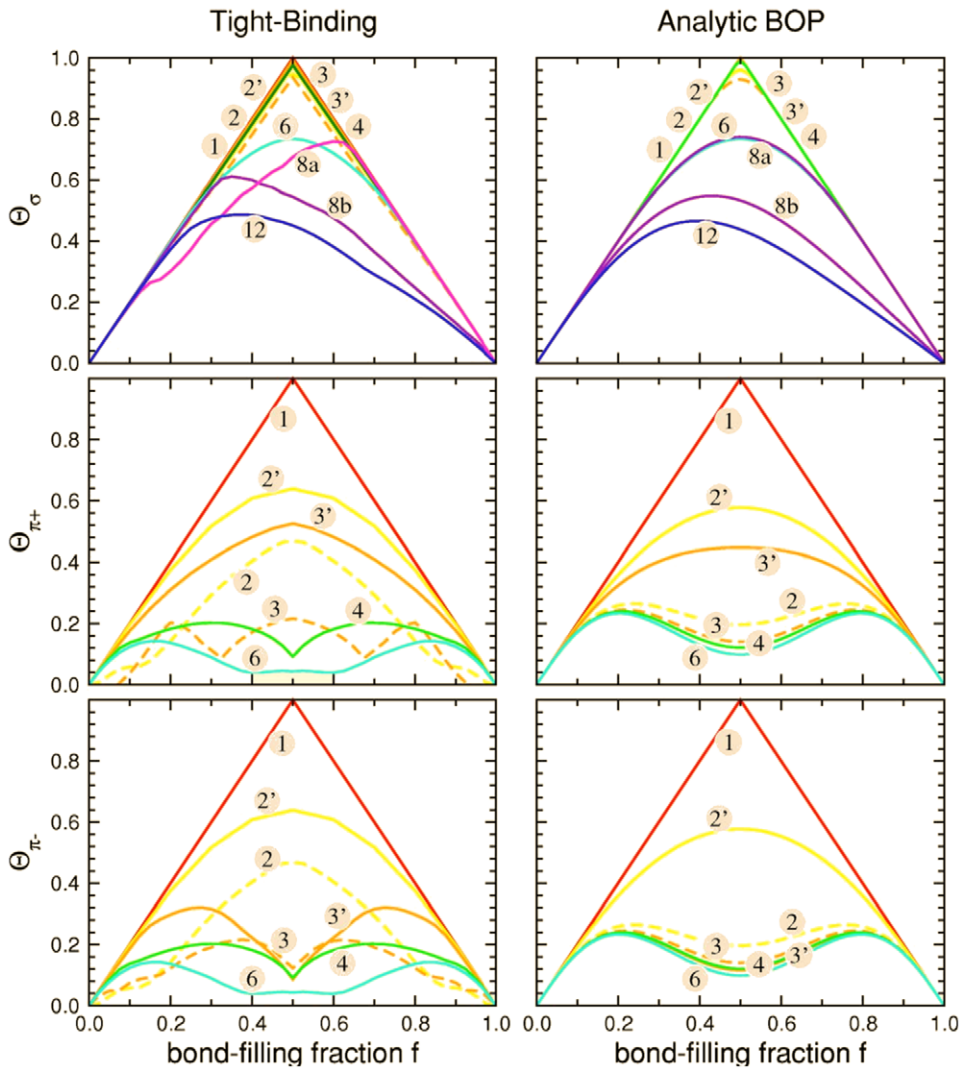

Figure 2. Bond order for σ and π bonds as a function of band filling for an orthogonal TB model that roughly corresponds to silicon. The numbers indicate the coordination of the structures, see text for details. Taken from [21].

elements only the ones that have the same angular quantum number m on both atoms will be different from zero,

$$\langle i\ l_i m_i|\hat{H}|j\ l_j m_j\rangle \neq 0 \quad \text{if } m_i = m_j \text{ and } m_i \leqslant l_i \text{ and } m_j \leqslant l_j\ . \tag{55}$$

For example, two s orbitals on atoms i and j can only form a σ bond, for an s orbital and a p orbital the same is true, while two p orbitals can form σ or π bonds, $p_z p_z \sigma$ and $p_x p_x \pi = p_y p_y\ \pi$. For s, p and d orbitals only the following matrix elements are different from zero in the two-centre approximation: $ss\sigma$, $sp\sigma$, $ps\sigma$, $pp\sigma$, $ds\sigma$, $sd\sigma$, $pd\sigma$, $dp\sigma$, $dd\sigma$, $pp\pi$, $pd\pi$, $dp\pi$, $dd\pi$, $dd\delta$. These matrix elements are often referred to as bond integrals. Even fewer matrix elements are different from zero if orbitals on the same atom are considered. Then

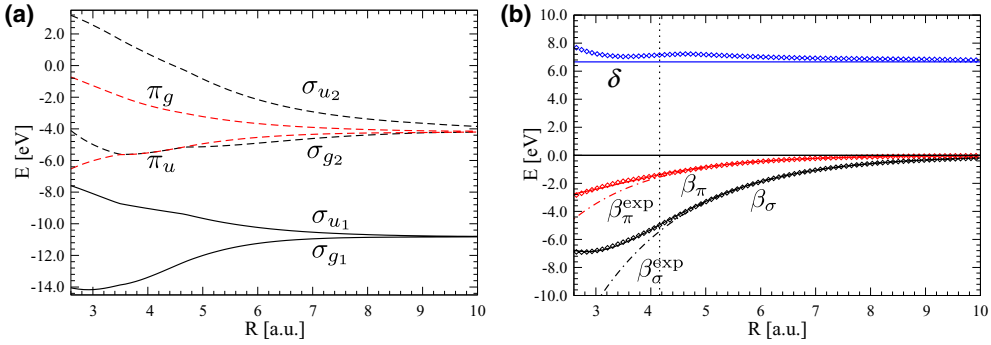

Figure 3. Distance dependence of the DFT eigenspectrum of a silicon dimer (*a*) and the corresponding orthogonal Hamiltonian matrix elements (*b*). Taken from [24].

$$\langle i\ l_1 m_1|\hat{H}|i\ l_2 m_2\rangle = E_{l_1}\delta_{l_1 l_2}\delta_{m_1 m_2}\,. \tag{56}$$

Thus in the two-centre approximation only three matrix elements E_s, E_p and E_d are required to characterize the matrix elements on a *spd*-valent atom. These diagonal elements of the Hamiltonian are usually referred to as onsite levels.

Figure 3 shows the DFT eigenspectrum of a Si dimer as a function of the distance between the atoms in the left-hand panel and the distance dependence of the corresponding orthogonal TB bond integrals β in the right-hand panel. The difference between the s and p onsite levels is given by $\delta = E_p - E_s$. For distances larger than the equilibrium distance that is marked with a vertical dotted line, the bond integrals are very well interpolated with exponential functions, while δ is indeed nearly constant.

It may seem that the two-centre approximation would be inaccurate in non-dimeric systems due to the general matrix element $\langle i\alpha|\hat{H}|j\beta\rangle$ being dependent on the presence of neighbouring atoms in the vicinity of the bond $i-j$. The influence of these three-centre integrals on the effective two-centre contribution is discussed explicitly in [25, 26]. In practice, however, the three-centre integrals are usually neglected as it has been found that a lot can be achieved within the simple two-centre approximation alone. In the following we will discuss the structure of the matrix elements beyond the two-centre approximation. For simplicity we will assume rigid basis functions that do not change with environment. The reference Hamiltonian $\boldsymbol{H}^{(0)}$ is obtained from overlapping atomic like charge densities. In other words, one assumes that the density matrix is diagonal,

$$n_{i\alpha j\beta} = N^{(0)}_{i\alpha}\delta_{i\alpha j\beta} \tag{57}$$

where $N^{(0)}_{i\alpha}$ denotes the number of electrons in the orbitals of the non-magnetic free atom i and where the occupation of all orbitals with the same angular momentum is identical so that the atomic charge distribution is spherical. Therefore the charge density equation (6) is written as

$$\rho = \sum_i \rho_i^{(0)}\,, \tag{58}$$

with

$$\rho_i^{(0)} = \sum_\alpha N^{(0)}_{i\alpha}\,|\varphi_{i\alpha}(\boldsymbol{r}-\boldsymbol{R}_i)|^2\,. \tag{59}$$

Then, using the expansion of the Hamiltonian in equation (32) we have

$$\boldsymbol{H}^{(0)} = \boldsymbol{T} + \boldsymbol{V}^{\mathrm{ext}} + \boldsymbol{V}^{\mathrm{XC}} + (\boldsymbol{J}^{\mathrm{H}} + \boldsymbol{J}^{\mathrm{XC}})\boldsymbol{n}^{(0)} + \frac{1}{2}\boldsymbol{K}\boldsymbol{n}^{(0)}\boldsymbol{n}^{(0)} + \cdots . \tag{60}$$

If the spherical charge density of the atomic core is denoted as $\rho_{i,\mathrm{nuc}}(\boldsymbol{r} - \boldsymbol{R}_i)$ and for the moment we neglect the contribution from exchange and correlation, then the matrix elements of the Hamiltonian are given by

$$H^{(0)}_{i\alpha j\beta} = T_{i\alpha j\beta} + \sum_k V^{(k)}_{i\alpha j\beta} , \tag{61}$$

with the matrix elements of the potential

$$V^{(k)}_{i\alpha j\beta} = \int \mathrm{d}\boldsymbol{r}\, \varphi_{i\alpha}(\boldsymbol{r} - \boldsymbol{R}_i)\, \varphi^*_{j\beta}(\boldsymbol{r} - \boldsymbol{R}_j)\, V_k(|\boldsymbol{r} - \boldsymbol{R}_k|) , \tag{62}$$

with

$$V_k(|\boldsymbol{r} - \boldsymbol{R}_k|) = \int \mathrm{d}\boldsymbol{r}'\, \frac{\rho^{(0)}_k(|\boldsymbol{r}' - \boldsymbol{R}_k|) + \rho_{k,\mathrm{nuc}}(|\boldsymbol{r}' - \boldsymbol{R}_k|)}{|\boldsymbol{r} - \boldsymbol{r}'|} , \tag{63}$$

and where the spherical nature of the atomic charge distributions was exploited. It is clear that the matrix elements can be written as functions of the interatomic distances between the atoms i, j and k,

$$V^{(k)}_{i\alpha j\beta} = V^{(k)}_{i\alpha j\beta}(R_{ij}, R_{ki}, R_{kj}) , \tag{64}$$

with the orbitals α and β oriented along the bond ij as in the two-centre approximation. The contributions to $\boldsymbol{H}^{(0)}$ with $i \neq j \neq k$ are three-centre integrals [25, 26]. Equation (61) also holds for the onsite levels

$$E^{(0)}_{i\alpha} = H^{(0)}_{i\alpha i\alpha} = T_{i\alpha i\alpha} + \sum_k V^{(k)}_{i\alpha i\alpha} , \tag{65}$$

where from equation (62) follows that $V^{(k)}_{i\alpha i\alpha}$ is a pairwise function

$$V^{(k)}_{i\alpha i\alpha} = V^{(k)}_{i\alpha i\alpha}(R_{ik}) , \tag{66}$$

such that the difference between the reference onsite levels $E^{(0)}_{i\alpha}$ and the atomic onsite levels $E^{(\mathrm{at})}_{i\alpha}$ is given by

$$E^{(0)}_{i\alpha} - E^{(\mathrm{at})}_{i\alpha} = \sum_k^{k\neq i} V^{(k)}_{i\alpha i\alpha}(R_{ik}) . \tag{67}$$

The functional dependence of equation (64) also holds if contributions from exchange and correlation up to second order are taken into account. Four-centre contributions to $\boldsymbol{H}^{(0)}$ must come from third-order expansion contributions of the exchange-correlation functional and are thus expected to be small. Furthermore, the TB orbitals on each atom change as a function of volume and environment, which may introduce a more complicated dependence of the matrix elements than the one discussed above.

Figure 4 shows the environmental dependence of the $ss\sigma$ bond integral in nickel [25]. A third atom k is placed next to the bond $i - j$. In the figure the distance R_{ij} is kept constant and the position of atom k is varied. The legend on the right-hand side gives the change of the bond

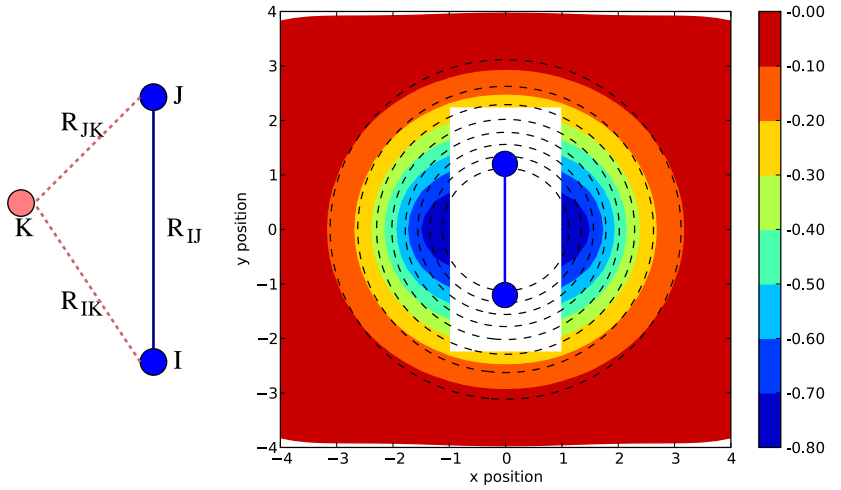

Figure 4. Environmental dependence of the effective two-centre bond integral $ss\sigma$ due to the presence of three-centre contributions in a non-orthogonal TB model of nickel [25].

integral in eV, the dashed lines are circles centred in the middle of the bond $i-j$. The data is desribed only approximately by the circles.

The discussion in this section was for non-orthgonal TB models only. In an orthogonal TB model the bond integrals are screened and therefore have a more significant dependence on the environment [27]. The screened orthogonal Hamiltonian matrix elements may be obtained following equation (20) as

$$\tilde{H}^{(0)}_{i\alpha j\beta} = H^{(0)}_{i\alpha j\beta} - \frac{1}{2}(H^{(0)}_{i\alpha k\gamma}\mathfrak{S}_{k\gamma j\beta} + \mathfrak{S}_{i\alpha k\gamma}H^{(0)}_{k\gamma j\beta}) + \frac{1}{4}\mathfrak{S}_{i\alpha k\gamma}H^{(0)}_{k\gamma l\delta}\mathfrak{S}_{l\delta j\beta}\,. \tag{68}$$

Figure 5 shows the environmental dependence of the σ bond integral in an orthogonal TB model of silicon [24]. The symbols mark data points obtained from minimal basis DFT, the solid lines show the distance dependence of the bond integrals in the different structure types. The dashed line shows the second-neighbour bond in bcc. The environmental dependence of the bond integrals is modelled using the lowest-order expansion equation (19) in equation (20). A more detailed derivation of the environmental dependence of the bond integrals in an orthogonal TB model may be found in [27].

3.3.2. The second-order contribution: charge transfer. It is often assumed that only the modification of the Mulliken charges contribute to the second-order term $\frac{1}{2}\boldsymbol{J}'\boldsymbol{\delta n}\boldsymbol{\delta n}$ and not the complete density matrix. These charges are given by equation (11),

$$q_{i\alpha} = N_{i\alpha} - N^{(0)}_{i\alpha} = \sum_{j\beta}\delta n_{i\alpha j\beta}S_{j\beta i\alpha}\,, \tag{69}$$

where the index 0 indicates the population of orbital $|i\alpha\rangle$ in a non-magnetic free atom. This requires that the four-centre second-order expansion coefficient is approximated in the following form [8],

$$J'_{i\alpha i'\alpha' j\beta j'\beta'} = J_{i\alpha j\beta}S_{i\alpha i'\alpha'}S_{j\beta j'\beta'} \tag{70}$$

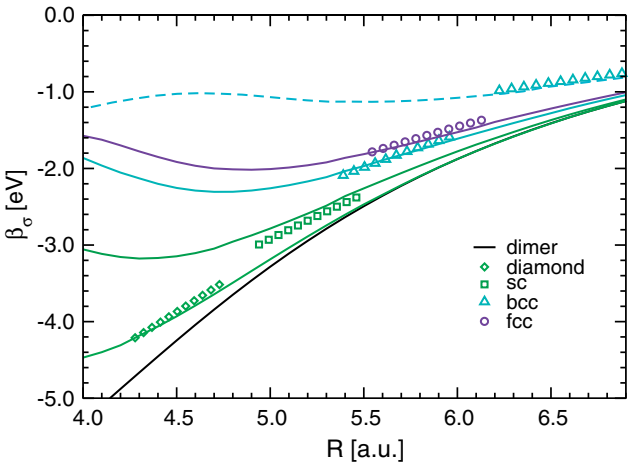

Figure 5. Environmental dependence of the Hamiltonian matrix elements in an orthogonal TB model of silicon [24].

where $J_{i\alpha j\beta}$ only depends on two orbitals $|i\alpha\rangle$ and $|j\beta\rangle$. This simplification has important implications for the structure of the TB model. From equations (41) and (42) the energy and the Hamiltonian are now given by

$$U = U^{(0)} + \sum_{i\alpha j\beta} H^{(0)}_{i\alpha j\beta} n_{j\beta i\alpha} + \sum_{i\alpha j\beta} \frac{1}{2} J_{i\alpha j\beta} q_{j\beta} q_{i\alpha} \,, \tag{71}$$

and

$$H_{i\alpha j\beta} = H^{(0)}_{i\alpha j\beta} + J_{i\alpha k\gamma} S_{i\alpha j\beta}\, q_{k\gamma} \,. \tag{72}$$

The modification of $\boldsymbol{H}^{(0)}$ may be simplified by introducing the onsite levels

$$E_{i\alpha} = E^{(0)}_{i\alpha} + J_{i\alpha k\gamma}\, q_{k\gamma} \,, \tag{73}$$

that are modified by the Mulliken charges away from their reference value $E^{(0)}_{i\alpha}$. This means that charge transfer only modifies the onsite matrix elements $E_{i\alpha}$ and leaves the rest of the Hamiltonian unchanged from its reference state $\boldsymbol{H}^{(0)}$

$$H_{i\alpha j\beta} = H^{(0)}_{i\alpha j\beta} + (E_{i\alpha} - E^{(0)}_{i\alpha}) S_{i\alpha j\beta} \,. \tag{74}$$

Multipole expansions are sometimes employed to represent the non-spherical character of the charges [11, 28–30]. This corresponds to an explicit parameterization of the angular dependence of $\boldsymbol{J}$ in the above equations.

Often a further approximation is made and it is assumed that only the total charge on each atom $q_i = \sum_\alpha q_{i\alpha}$ enters the energy as the second-order term takes the form $\sum_{ij} \frac{1}{2} J_{ij} q_i q_j$. From equation (72) it is clear that in this case all onsite levels on an atom are shifted in parallel upon charge transfer.

A formal treatment of the electrostatic contributions associated to charge transfer without making *ad hoc* approximations requires the full evaluation of the four-centre integrals equation (28) as in general the density matrix cannot be assumed to be diagonal. Magnetic terms follow in complete analogy but are short ranged as they only enter the energy through the

exchange-correlation functional. A non-linear dependence of the Hamiltonian on $\boldsymbol{n}$ is introduced if third-order contributions from the exchange-correlation energy are also taken into account.

3.3.3. The zeroth-order contribution: repulsive energy. The zeroth-order contribution, i.e. the reference energy that is independent of $\delta\boldsymbol{n}$, is often parameterized with pairwise functions. A more detailed discussion of the zeroth-order contribution will follow in section 4.5 after the TB bond model has been introduced and the character of the repulsive energy is clearer.

4. The TB bond model

In the following we will show that the second-order expansion of the DFT energy equation (41) of a non-magnetic material with respect to the energy of non-magnetic free atoms, namely the non-magnetic binding or cohesive energy, may be written as

$$U_\mathrm{B} = U - U_\mathrm{free\,atoms} = U_\mathrm{bond} + U_\mathrm{prom} + U_\mathrm{ion} + U_\mathrm{es} + U_\mathrm{rep}\,, \tag{75}$$

where each of the terms will now be discussed. This expression for the binding energy is called the TB bond model [7, 8]. For each contribution to the binding energy we will first discuss its general form in a non-orthogonal TB model and then give the expression for an orthogonal TB model.

4.1. Bond energy

The bond energy summarizes the energy that is stored in the bonds between different atoms

$$\begin{aligned} U_\mathrm{bond} &= \sum_{i\alpha j\beta} \left(H_{i\alpha j\beta} - \frac{1}{2}(E_{i\alpha} + E_{j\beta}) S_{i\alpha j\beta} \right) n_{j\beta i\alpha} \\ &= U_\mathrm{band} - \sum_{i\alpha} E_{i\alpha} N_{i\alpha}\,, \end{aligned} \tag{76}$$

with the band energy $U_\mathrm{band} = \boldsymbol{Hn}$. We introduce the bond integrals [12, 26]

$$\beta_{i\alpha j\beta} = H_{i\alpha j\beta} - \frac{1}{2}(E_{i\alpha} + E_{j\beta}) S_{i\alpha j\beta}\,. \tag{77}$$

that make it explicitly clear that the bond energy only involves bonds between different atoms,

$$U_\mathrm{bond} = \sum_{i\alpha j\beta}^{i\alpha \neq j\beta} \beta_{i\alpha j\beta} n_{j\beta i\alpha}\,. \tag{78}$$

This representation of the bond energy is usually referred to as the *intersite* representation. Different from the band energy $\boldsymbol{Hn}$, the bond energy is invariant with respect to a shift of the energy scale. Using equation (72) the bond energy is closely related to the linear term in the TB energy

$$\boldsymbol{H}^{(0)}\boldsymbol{n} = U_\mathrm{bond} + \sum_{i\alpha} E^{(0)}_{i\alpha} N_{i\alpha}\,. \tag{79}$$

Equivalent to the intersite representation is the *onsite* representation of the bond energy:

$$U_{\text{bond}} = \sum_{i\alpha} \int_{-\infty}^{E_{\text{F}}} (E - E_{i\alpha}) n_{i\alpha}(E)\, \mathrm{d}E, \tag{80}$$

with the local density of states

$$n_{i\alpha}(E) = \frac{\mathrm{d}N_{i\alpha}}{\mathrm{d}E}\,, \tag{81}$$

and the Fermi level E_{F}.

In the onsite representation one sees that the population of the density of states below $E_{i\alpha}$ leads to a negative contribution to the bond energy, i.e. corresponding to bonding states. Once states above $E_{i\alpha}$ have to be populated, the bond energy decreases, corresponding to a filling of anti-bonding states. The integral over the complete band always results in zero, $0 = U_{\text{bond}} = \sum_{i\alpha} \int_{-\infty}^{\infty} (E - E_{i\alpha}) n_{i\alpha}(E)\, \mathrm{d}E$, which helps to show that the bond energy is always smaller or equal to zero,

$$U_{\text{bond}} \leqslant 0\,. \tag{82}$$

The proof for this inequality just requires that the derivative of the bond energy, $(E - E_{i\alpha})$ $n_{i\alpha}(E)$, can cross zero only once at $E = E_{i\alpha}$ as the density of states fulfills $n_{i\alpha}(E) \geqslant 0$. From equation (80) one can also view the bond energy for each orbital $|i\alpha\rangle$ as the band energy of the atom centered on $E_{i\alpha}$.

4.1.1. Orthogonal TB model. In an orthogonal TB model the Hamiltonian matrix is screened, equation (68) and the bond energy may be written as

$$U_{\text{bond}} = \sum_{i\alpha j\beta}^{i\alpha \neq j\beta} \tilde{H}_{i\alpha j\beta} n_{j\beta i\alpha}\,. \tag{83}$$

The diagonal elements of the orthogonal TB Hamiltonian $\tilde{\boldsymbol{H}}^{(0)}$ are given explicitly as

$$\begin{aligned} \tilde{E}^{(0)}_{i\alpha} = E^{(0)}_{i\alpha} &- \frac{1}{2} \sum_{k\gamma} (H_{i\alpha k\gamma} \mathfrak{S}_{k\gamma i\alpha} + \mathfrak{S}_{i\alpha k\gamma} H_{k\gamma i\alpha}) \\ &+ \frac{1}{4} \sum_{k\gamma l\delta} \mathfrak{S}_{i\alpha k\gamma} H_{k\gamma l\delta} \mathfrak{S}_{l\delta i\alpha}\,, \end{aligned} \tag{84}$$

such that we have for an orthogonal model

$$\tilde{\boldsymbol{H}}^{(0)} \boldsymbol{n} = U_{\text{bond}} + \sum_{i\alpha} \tilde{E}^{(0)}_{i\alpha} N_{i\alpha}\,. \tag{85}$$

The screening of the Hamiltonian matrix is to some extent cancelled by three-centre contributions in the non-orthogonal TB model, so that the environmental dependence of the matrix elements in orthogonal TB models is often surprisingly small.

4.2. Promotion energy

The promotion energy is associated with the re-population of the onsite levels when bonds are formed. In the free atom reference state the number of electrons per orbital is $N^{(0)}_{i\alpha}$. For charge neutral atoms the promotion energy is then written as

$$U_{\text{prom}} = \sum_{i\alpha} E^{(0)}_{i\alpha}(N_{i\alpha} - N^{(0)}_{i\alpha}) \,. \tag{86}$$

As the electrons in the free atom state occupy the energetically lowest orbitals, the promotion energy is expected to be positive, in contrast to the bond energy. With the promotion energy, the linear term in the DFT expansion equation (41) now becomes

$$\boldsymbol{H}^{(0)}\boldsymbol{n} = U_{\text{bond}} + U_{\text{prom}} + \sum_{i\alpha} E^{(0)}_{i\alpha} N^{(0)}_{i\alpha} \,, \tag{87}$$

where $\sum_{i\alpha} N^{(0)}_{i\alpha} E^{(0)}_{i\alpha}$ is a constant offset that we will take care of in the calculation of the binding energy.

4.2.1. Orthogonal TB model. In an orthogonal TB model, the promotion energy is computed with the screened onsite levels of equation (84)

$$U_{\text{prom}} = \sum_{i\alpha} \tilde{E}^{(0)}_{i\alpha}(N_{i\alpha} - N^{(0)}_{i\alpha}) \,, \tag{88}$$

so that equation (87) also holds for orthogonal models,

$$\tilde{\boldsymbol{H}}^{(0)}\boldsymbol{n} = U_{\text{bond}} + U_{\text{prom}} + \sum_{i\alpha} \tilde{E}^{(0)}_{i\alpha} N^{(0)}_{i\alpha} \,. \tag{89}$$

4.3. Free atom energy

For the evaluation of the binding energy we subtract the energies of non-magnetic free atoms from the TB energy

$$U_{\text{B}} = U^{\text{TB}} - U^{\text{TB}}_{\text{free atoms}} \,. \tag{90}$$

From equation (71) the TB energy of non-magnetic, charge neutral free atoms is given by

$$U^{\text{TB}}_{\text{free atoms}} = \sum_{i\alpha} E^{(\text{at})}_{i\alpha} N^{(0)}_{i\alpha} - \frac{1}{2} \sum_{i\alpha\beta} J_{i\alpha i\beta} N^{(0)}_{i\alpha} N^{(0)}_{i\beta} \,, \tag{91}$$

where $E^{(\text{at})}_{i\alpha}$ are the eigenstates of the free atom i and the population of the atomic orbitals is equal to the population in the reference state, $N^{(0)}_{i\alpha}$.

4.4. Preparation energy

We complete the discussion of the linear term in the TB model by introducing the preparation energy

$$U_{\text{prep}} = \sum_{i\alpha} (E^{(0)}_{i\alpha} - E^{(\text{at})}_{i\alpha}) N^{(0)}_{i\alpha} \,. \tag{92}$$

The preparation energy accounts for the change in atomic onsite levels from $E^{(\text{at})}_{i\alpha}$ to $E^{(0)}_{i\alpha}$ when the free atom charge densities are overlapped to form the TB reference charge density. The linear contribution to the binding energy is now written as

$$\boldsymbol{H}^{(0)}\boldsymbol{n} - E^{(\text{at})}_{i\alpha} N^{(0)}_{i\alpha} = U_{\text{bond}} + U_{\text{prom}} + U_{\text{prep}} \,. \tag{93}$$

4.4.1. Orthogonal TB model. Following equation (84) the preparation energy in an orthogonal TB model is written as

$$U_{\text{prep}} = \sum_{i\alpha} (\tilde{E}^{(0)}_{i\alpha} - E^{(\text{at})}_{i\alpha}) N^{(0)}_{i\alpha} = \sum_{i\alpha} (E^{(0)}_{i\alpha} - E^{(\text{at})}_{i\alpha}) N^{(0)}_{i\alpha} + U_{\text{overlap}} \,, \tag{94}$$

with the overlap repulsion

$$U_{\text{overlap}} = -\frac{1}{2} \sum_{i\alpha} \left[\sum_{j\beta} (H_{i\alpha j\beta} \mathfrak{S}_{j\beta i\alpha} + \mathfrak{S}_{i\alpha j\beta} H_{j\beta i\alpha}) - \frac{1}{4} \sum_{k\gamma l\delta} \mathfrak{S}_{i\alpha k\gamma} H_{k\gamma l\delta} \mathfrak{S}_{l\delta i\alpha} \right] N^{(0)}_{i\alpha} \,. \tag{95}$$

The overlap repulsion typically dominates the repulsive interaction in an orthogonal TB model.

4.5. Repulsive energy

The repulsive energy summarizes all terms that do no explicitly depend on $\delta \boldsymbol{n}$. For this reason U_{prep} is also absorbed in the repulsive energy

$$U_{\text{rep}} = -\frac{1}{2} \sum_{i\alpha j\beta}^{j\neq j} J_{i\alpha j\beta} N^{(0)}_{i\alpha} N^{(0)}_{j\beta} + U_{\text{nuc}} + U_{\text{prep}} \,. \tag{96}$$

The sum $-\frac{1}{2} \sum_{i\alpha j\beta}^{j\neq j} J_{i\alpha j\beta} N^{(0)}_{i\alpha} N^{(0)}_{j\beta} + U_{\text{nuc}}$ is expected to be strictly positive, so that the repulsive energy is positive overall. The preparation energy contains the overlap repulsion which is the main repulsive contribution in an orthogonal TB model.

A more detailed discussion of equation (96) can be made by assuming rigid atomic-like basis functions. Because of the spherical atomic-like charge distribution on each atom in the reference state, the explicit electrostatic contribution is exactly pairwise and may be written as

$$\begin{aligned} \Phi_{ij}(R_{ij}) &= -\sum_{\alpha\beta} J^{(H)}_{i\alpha j\beta} N^{(0)}_{i\alpha} N^{(0)}_{j\beta} + U_{\text{nuc},ij} \\ &= \int \mathrm{d}\boldsymbol{r} \int \mathrm{d}\boldsymbol{r}' \, \frac{\rho_{i,\text{nuc}}(|\boldsymbol{r} - \boldsymbol{R}_i|)\rho_{j,\text{nuc}}(|\boldsymbol{r}' - \boldsymbol{R}_j|) - \rho^{(0)}_i(|\boldsymbol{r} - \boldsymbol{R}_i|)\rho^{(0)}_j(|\boldsymbol{r}' - \boldsymbol{R}_j|)}{|\boldsymbol{r} - \boldsymbol{r}'|} \,, \end{aligned} \tag{97}$$

with $i \neq j$. This pairwise interaction is different from zero only if the atoms are close enough for that their charge densities overlap. If the atoms are further apart the electrostatic interaction of the spherical atomic charge densities is exactly cancelled by the electrostatic repulsion of the nuclei.

The electrostatic contribution to the preparation energy may be obtained from equation (67), such that

$$U_{\text{prep}} = \frac{1}{2} \sum_{ij}^{i\neq j} \Phi_{ij,\text{prep}}(R_{ij}) \,, \tag{98}$$

with the pairwise function

$$\Phi_{ij,\text{prep}}(R_{ij}) = \frac{1}{2} \left[\sum_{\alpha} V^{(j)}_{i\alpha i\alpha} N^{(0)}_{i\alpha} + \sum_{\beta} V^{(i)}_{j\beta j\beta} N^{(0)}_{j\beta} \right]. \tag{99}$$

Even when contributions up to second-order from exchange and correlation are included, the repulsive energy in a non-orthogonal TB model may be written as a strictly pairwise function

$$U_{\text{rep}} = \frac{1}{2} \sum_{ij}^{j \neq j} \left[\Phi_{ij}(R_{ij}) + \Phi_{ij,\text{prep}}(R_{ij}) \right] . \tag{100}$$

The pairwise form of the repulsive energy is only broken by third or higher-order contributions from exchange and correlation. The non-pairwise terms are therefore expected to be small. Clearly, when the basis functions are not rigid and are allowed to adapt to the local environment, this will bring in contributions that are not pairwise, too.

4.5.1. Orthogonal TB model. The overlap repulsion needs to be added for an orthogonal TB model. The overlap repulsion is pairwise only to lowest order. Therefore, in situations where atomic orbitals overlap significantly, i.e. when atoms are at close distance, the overlap repulsion will contribute to non-pairwise interactions in the repulsive energy of orthogonal TB models [26].

4.6. Charge transfer

So far we have not discussed charge transfer and implicitly assumed that the atoms remain charge neutral when bonds are formed. If charge transfer is allowed, two further contributions to the energy arise (and the expression for the promotion energy is somewhat modified): (i) an energy linear in charge due to the onsite level difference between atoms and (ii) the second-order contributions to the TB energy given in equation (71). The two contributions are given by the electrostatic interaction of charges on different atoms

$$U_{\text{es}} = \frac{1}{2} \sum_{ij}^{i \neq j} J_{ij} q_i q_j , \tag{101}$$

and an ionic onsite contribution that characterizes the energy associated with charging each atom

$$U_{\text{ion}} = \bar{E}_i q_i + \frac{1}{2} \sum_i J_{ii} q_i^2 , \tag{102}$$

The energy $\bar{E}_i$ is obtained as a weighted average of the reference onsite levels on atom i and corresponds to the electronegativity of the atom. The term J_{ii} is strictly positive for resistance against charge transfer from the charge neutral state and is sometimes labeled U to make reference to Hubbard's work [31].

4.7. Summary of the binding energy

Modern TB is derived from DFT and supersedes some older TB approaches that we could not discuss here. The second-order expansion of DFT, equation (41), may be re-written in the TB bond model as

$$U_{\text{B}} = U_{\text{bond}} + U_{\text{prom}} + U_{\text{ion}} + U_{\text{es}} + U_{\text{rep}} . \tag{103}$$

If charge transfer can be neglected, the contributions to U_{B} linear in $\boldsymbol{n}$ are given by $U_{\text{bond}} + U_{\text{prom}} + U_{\text{prep}}$, equation (93). The preparation energy contains the overlap repulsion and is absorbed in the repulsive energy U_{rep}. If charge transfer cannot be neglected, the ionic and electrostatic contribution, $U_{\text{ion}} + U_{\text{es}}$, will be different from zero. This representation of the energy contains the contributions of the second-order expansion of the DFT functional, equation (41).

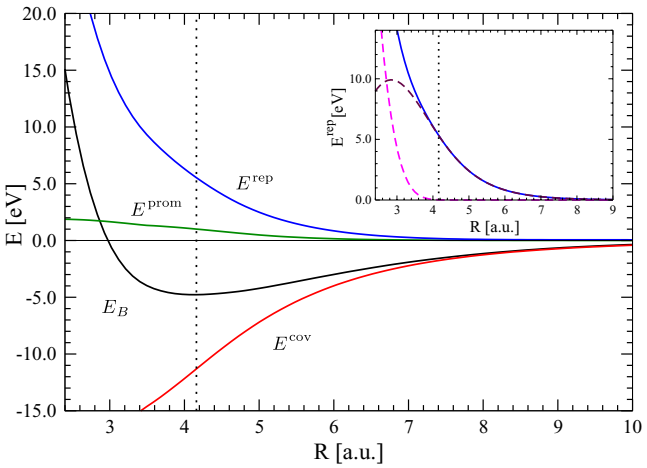

Figure 6. Different contributions to the binding energy of a Si dimer. $E_{\rm cov}$ corresponds to the covalent bond energy $U_{\rm bond}$. The dotted vertical line indicates the equilibrium bond distance. From [24].

This expansion suggests a representation of bond formation in the following steps:

1.	$U_{\rm rep}$	→ overlap atomic charge densities	> 0
2.	$U_{\rm ion}$	→ charge atoms	> 0
3.	$U_{\rm prom}$	→ re-populate atomic energy levels	> 0
4.	$U_{\rm bond} + U_{\rm es}$	→ chemical and electrostatic interactions	< 0

Steps 1-3 prepare the atoms for bonding and are typically associated with an increase in energy as they perturb the free atom state. The formation of chemical bonds and electrostatic interactions in step 4 lead to a lowering of the energy and are the driving force for bonding in materials and molecules.

The focus in TB theory is today on a more systematic characterization of the approximations that we have summarized in section 3. A particular focus is on the parameterization of the matrix elements $\boldsymbol{H}^{(0)}$ and partly on $\boldsymbol{J}$ as well as improved expressions and parameterizations for $U_{\rm rep}$.

4.8. Example: TB energy of the silicon dimer

Figure 6 shows the different contributions to the TB energy for a silicon dimer in an orthogonal TB model. Bond formation is driven by the bond energy that in the figure is abbreviated as $E^{\rm cov}$. The other two contributions to the binding energy, the promotion energy and the repulsive energy, are both positive. For distances larger than approximately the equilibrium distance the repulsive energy is well approximated by the overlap repulsion. At shorter distances other contributions from the repulsive energy become important, too. As the atoms in the dimer are charge neutral, contributions from charge transfer vanish.

5. Bond-order potentials

The bond-order potentials correspond to a local expansion of the solution of an orthogonal TB model. The expansion parameter—the number of moments taken into account in the

expansion—determines how closely the BOPs approach the TB solution and how computationally intensive they are. If only a few moments are taken into account, the BOPs are efficient interatomic potentials. If a large number of moments is considered for the expansion, the BOPs represent an accurate $O(N)$ solution of the TB problem.

The development of the bond-order potentials started 25 years ago [32]. The analytic BOPs for transition metals were mainly developed in [8, 33]. The energies provided by the analytic BOPs are numerically close to the so-called numerical BOPs [34, 35], while the analytic BOPs also provide exact force gradients. A comparison of numerical and analytic BOPs may be found in [36, 37]. The analytic BOPs build on moments methods and the recursion expansion [38] and may be linked [39] to the kernel-polynomial method (KPM) [40–42] and the Fermi operator expansion (FOE) [43, 44].

In the following we will restrict our discussion to non-magnetic bond-order potentials. The BOPs may be extended to include magnetism, the magnetic BOPs are discussed in detail in [8, 45, 46]. Also we will not discuss the analytic bond-based bond-order potentials that have been derived for *sp*-valent materials [19, 20].

5.1. Moments and moments expansion

The local expansion of the solution of the TB model in the BOPs is based on the following observation. In an orthogonal TB model, the moments of the density of states may be obtained by evaluating self-returning hopping paths

$$\begin{aligned}\mu_{i\alpha}^{(n)} &= \int E^n n_{i\alpha}(E)\,\mathrm{d}E = \langle i\alpha|\hat{H}^n|i\alpha\rangle \\ &= H_{i\alpha j\beta}H_{j\beta k\gamma}H_{k\gamma\ldots}\ldots H_{\ldots i\alpha}\,,\end{aligned} \tag{104}$$

where the second line comprises $n-1$ multiplications of n Hamiltonian matrices. The zeroth moment corresponds to the norm

$$\mu_{i\alpha}^{(0)} = \int n_{i\alpha}\,\mathrm{d}E = 1\,, \tag{105}$$

while the first moment is the centre of gravity of the local density of states, which is given by the onsite levels

$$\mu_{i\alpha}^{(1)} = \int E n_{i\alpha}\,\mathrm{d}E = E_{i\alpha}\,. \tag{106}$$

The lowest moment that contains information about the environment of atom i is the second moment. The second moment characterizes the root mean square width of the local density of states

$$\mu_{i\alpha}^{(2)} = \int E^2 n_{i\alpha}\,\mathrm{d}E\,. \tag{107}$$

The third moment and fourth moment together with the second moment allow one to evaluate the skewness and the bimodality of the density of states,

$$\mu_{i\alpha}^{(3)} = \int E^3 n_{i\alpha}\,\mathrm{d}E\,, \qquad \mu_{i\alpha}^{(4)} = \int E^4 n_{i\alpha}\,\mathrm{d}E\,. \tag{108}$$

The higher moments contain more detailed information of the structure of $n_{i\alpha}$.

If the moments are known, one should be able to reconstruct the local density of states $n_{i\alpha}(E)$. In practice, the reconstruction of the density of states is formally equivalent to a Fourier

series expansion. We start by changing the energy scale in such a way that the density of states is contained in the interval from -1 to $+1$. To this end we introduce two new variables, a_∞ and b_∞. The two variables are chosen in such a way that the density of states is zero below $a_\infty - 2\,b_\infty$ and above $a_\infty + 2\,b_\infty$, or, in other words, all eigenvalues are between $a_\infty - 2\,b_\infty$ and $a_\infty + 2\,b_\infty$. In practice the values of a_∞ and b_∞ may be estimated from the Hamiltonian [39]. Then, if we introduce

$$\epsilon = \frac{E - a_\infty}{2b_\infty}\,, \tag{109}$$

and

$$n_{i\alpha}(\epsilon) = 2b_\infty n_{i\alpha}(E)\,, \tag{110}$$

the re-scaled density of states $n_{i\alpha}(\epsilon)$ is contained in the interval -1 to $+1$. This allows us to work with Chebyshev polynomials that are defined on the same interval. Here we work with the Chebyshev polynomials of the second kind. The Chebyshev polynomials of the second kind fulfill the recursion relation

$$P_{n+1}(\epsilon) = 2\epsilon P_n(\epsilon) - P_{n-1}(\epsilon)\,, \tag{111}$$

with $P_0 = 1$ and $P_2 = 2\epsilon$. The polynomials are orthogonal with respect to the square root function

$$\frac{2}{\pi}\int_{-1}^{+1} P_n(\epsilon)P_m(\epsilon)\sqrt{1-\epsilon^2}\,\mathrm{d}\epsilon = \delta_{nm}\,. \tag{112}$$

If one introduces the phase $\epsilon = -\cos\phi$, then the Chebyshev polynomials correspond to the sine function

$$P_n(\epsilon) = \frac{\sin(n+1)\phi}{\sin\phi}\,. \tag{113}$$

The orthogonality of the Chebyshev polynomials may now be used to obtain expansion coefficients for the density of states by projection,

$$\sigma_{i\alpha}^{(n)} = \int_{-1}^{+1} P_n(\epsilon)n_{i\alpha}(\epsilon)\,\mathrm{d}\epsilon\,. \tag{114}$$

This equation may be easily validated by assuming that the density of states has been expanded in the form

$$n_{i\alpha}(\epsilon) = \sum_n \frac{2}{\pi}\sqrt{1-\epsilon^2}\,\sigma_{i\alpha}^{(n)}\,P_n(\epsilon)\,. \tag{115}$$

The expansion coefficients $\sigma_{i\alpha}^{(n)}$ may be obtained from the moments theorem equation (104) as

$$\sigma_{i\alpha}^{(n)} = \langle i\alpha|P_n(\hat{h})|i\alpha\rangle\,, \tag{116}$$

with the re-scaled Hamiltonian

$$\hat{h} = \frac{\hat{H} - a_\infty}{2b_\infty}\,. \tag{117}$$

Then by writing the Chebyshev polynomials explicitly as a polynomial in $\hat{h}$ and using the moments theorem, the expansion coefficients $\sigma_{i\alpha}$ are obtained.

5.2. Termination of the expansion

In practice only a certain number $n_{\max}$ of expansion coefficients (corresponding to $n_{\max}$ moments of the density of states) are computed. Depending on the application these are typically 4, 9 or 12 moments. Thus the expansion equation (115) becomes

$$n_{i\alpha}(\epsilon) = \sum_{n=0}^{n_{\max}} \sqrt{1-\epsilon^2}\,\sigma_{i\alpha}^{(n)} P_n(\epsilon)\,, \tag{118}$$

or using $\epsilon = -\cos\phi$,

$$n_{i\alpha}(\epsilon) = \sum_{n=0}^{n_{\max}} \sigma_{i\alpha}^{(n)} \sin(n+1)\phi\,. \tag{119}$$

If a Fourier series expansion is abruptly terminated because only the first $n_{\max}$ expansion coefficients are taken into account, this may lead to significant oscillations that are known as Gibbs ringing. In particular, these oscillations may be so large that the expansion of the density of states equation (119) may become negative. Negative values of the density of states are of course physically and mathematically incorrect and need to be avoided.

The Gibbs ringing may be removed and a strictly positive expansion of the density of states may be enforced by damping the expansion coefficients,

$$n_{i\alpha}(\epsilon) = \sum_{n=0}^{n_{\max}} g_n \sigma_{i\alpha}^{(n)} \sin(n+1)\phi\,. \tag{120}$$

The damping factors g_n decrease monotonically from $g_0 = 1$ to $g_{n_{\max}} = 0$ [39, 40]. In this way they damp the fast oscillations and avoid Gibbs ringing and potentially negative values of the density of states. On the other hand, because the damping factors decrease to zero for $n_{\max}$, they remove most of the contribution from higher moments. Thus, when using damping factors more moments need to be calculated, i.e. $n_{\max}$ needs to be increased. As, however, the calculation of the moments is the most time consuming part in the energy and force evaluation, one would like to keep $n_{\max}$ as small as possible.

This problem may be resolved by terminating the expansion equation (120), which means the following. One computes the first $n_{\max}$ moments from the Hamiltonian. Further moments from $n_{\max}+1$ up to $n_{\exp} \gg n_{\max}$ are then computed using an estimated model Hamiltonian that has the form of a semi-infinite chain with nearest-neighbour bonds only [39]. Because the topology of the semi-infinite chain is so simple, only very few matrix elements need to be multiplied for evaluating the moments and therefore the computation of the moments is very fast. This leads to an expansion in the form

$$n_{i\alpha}(\epsilon) = \sum_{n=0}^{n_{\max}} g_n \sigma_{i\alpha}^{(n)} \sin(n+1)\phi + \sum_{n=n_{\max}+1}^{n_{\exp}} g_n \sigma_{i\alpha}^{(n)} \sin(n+1)\phi\,. \tag{121}$$

The damping factors decay monotonically from $g_0 = 1$ to $g_{n_{nexp}} = 0$. If $n_{\exp} \gg n_{\max}$, the contributions from the first few moments are hardly damped such that an expansion is obtained that converges quickly to the TB reference density of states. Typical values for $n_{\exp}$ are 10–$20 \times n_{\max}$. This leads to a good quality of the reconstructed DOS already at a small number of calculated moments.

5.3. Bond energy

The expansion equation (121) may be integrated analytically, leading to

$$U_{\mathrm{bond},i\alpha} = 2b_\infty \sum_{n=0}^{n_{\mathrm{exp}}} g_n \sigma_{i\alpha}^{(n)} [\hat{\chi}_{n+2}(\phi_\mathrm{F}) - \gamma_0 \hat{\chi}_{n+1}(\phi_\mathrm{F}) + \hat{\chi}_n(\phi_\mathrm{F})] \,, \tag{122}$$

for the bond energy that orbital $i\alpha$ contributes, with $\gamma_0 = (E_{i\alpha} - a_\infty)/b_\infty$ and $\hat{\chi}_0 = 0$,

$$\hat{\chi}_1 = 1 - \frac{\phi_\mathrm{F}}{\pi} + \frac{1}{2\pi} \sin(2\phi_\mathrm{F}) \,, \tag{123}$$

and where for $n \geqslant 2$ the dimensionless response functions take the form

$$\hat{\chi}_n(\phi_\mathrm{F}) = \frac{1}{\pi} \left[\frac{\sin(n+1)\phi_\mathrm{F}}{n+1} - \frac{\sin(n-1)\phi_\mathrm{F}}{n-1} \right] . \tag{124}$$

The number of electrons in orbital $N_{i\alpha}$ is obtained as

$$N_{i\alpha} = 2 \sum_{n=0}^{n_{\mathrm{exp}}} \sigma_{i\alpha}^{(n)} \hat{\chi}_{n+1}(\phi_\mathrm{F}) \,. \tag{125}$$

The Fermi phase is given by $\epsilon_\mathrm{F} = -\cos\phi_\mathrm{F}$. It is determined by summing the number of electrons in all orbitals computed from equation (125), which has to match the total number of electrons in the system.

With $U_{\mathrm{bond},i\alpha}$ and the number of electrons $N_{i\alpha}$, the binding energy U_B, equation (103), may be now computed using the analytic BOPs.

5.3.1. Magnetism. The TB model and the BOP expansion may be extended to include collinear and non-collinear magnetism [8, 45, 46]. This requires that for every orbital two expansions of the density of states are carried out, one for the up-spin state, the other for the down-spin state. Consequently the bond energy and the number of electrons are evaluated separately for up and down spin bands, $U^{\uparrow}_{\mathrm{bond},i\alpha}$ and $U^{\downarrow}_{\mathrm{bond},i\alpha}$, $N^{\uparrow}_{i\alpha}$ and $N^{\downarrow}_{i\alpha}$. The number of electrons in orbital $i\alpha$ is given by

$$N_{i\alpha} = N^{\uparrow}_{i\alpha} + N^{\downarrow}_{i\alpha} \,, \tag{126}$$

and the magnitude of the magnetic moment is given by

$$m_{i\alpha} = N^{\uparrow}_{i\alpha} - N^{\downarrow}_{i\alpha} \,. \tag{127}$$

5.4. Energy calculation and self-consistency

The expression for the binding energy U_B, equation (103), is a function of the atomic positions $\boldsymbol{R}_i$ and the onsite levels $E_{i\alpha}$ for all $i = 1, \ldots, N$ atoms as well as the Fermi level E_F, where the Fermi level is determined from the total number of electrons in the material,

$$U_\mathrm{B} = U_\mathrm{B}(\boldsymbol{R}_i, E_{i\alpha}, E_\mathrm{F}) \,. \tag{128}$$

The energy is computed by minimizing U_B with respect to the onsite levels $E_{i\alpha}$ following equation (47). For a stationary point the derivatives need to vanish,

$$\frac{\partial U_\mathrm{B}}{\partial E_{i\alpha}} = 0 \,. \tag{129}$$

This condition is equivalent to self-consistency that in most TB or DFT calculations is achieved through self-consistent iteration, see sections 2.4 and 2.5. In the BOPs the self-consistent iteration cannot be used as the eigenspectrum of the Hamiltonian is approximated and therefore the direct variational minimization of the energy has to be achieved through equation (129) [8]. The evaluation of the derivatives required in equation (129) is closely related to the computation of forces and will be discussed in the next section.

5.5. Forces, stress and magnetic torques

The expansion of the energy in section 5.3 represents the binding energy U_B as a function of the local moments of the density of states and the Fermi level. When an atom is slightly displaced, some of the moments will also slightly change and so will the Fermi level. As the total number of electrons in the system remains constant, the change in the Fermi level may be computed from the change in moments. Furthermore, as the moments are functions of the Hamiltonian matrix elements, the expression for forces, stress and magnetic torques may be obtained by making use of the derivative

$$\tilde{\Theta}_{i\alpha j\beta} = \frac{\partial U_\mathrm{B}}{\partial H_{i\alpha j\beta}} \,. \tag{130}$$

The analytic form of $\tilde{\Theta}_{i\alpha j\beta}$ is derived in detail in [8]. Before the forces may be evaluated, the energy needs to be minimized with respect to the onsite levels $E_{i\alpha}$. Using equation (130) the condition equation (129) means that the diagonal elements of $\tilde{\boldsymbol{\Theta}}$ need to vanish

$$\tilde{\Theta}_{i\alpha i\alpha} = 0 \,, \tag{131}$$

where in this formulation charge conservation has been taken into account in the definition of $\tilde{\boldsymbol{\Theta}}$. This is in contrast to many TB or DFT implementations where a Lagrange multiplier is used to ensure that the total number of electrons is kept constant. The force on atom k is obtained by making use of the chain rule [8, 45],

$$\boldsymbol{F}_k = -\nabla_k U_\mathrm{B} = -\sum_{i\alpha j\beta}^{i\alpha \neq j\beta} \tilde{\Theta}_{i\alpha j\beta} \nabla_k H_{i\alpha j\beta} - \nabla_k U_\mathrm{rep} \,. \tag{132}$$

If the TB problem is solved exactly, this expression corresponds to the Hellmann–Feynman forces [47, 48] and $\tilde{\boldsymbol{\Theta}}$ becomes the bond-order or density matrix. As the BOPs approximate the TB solution, the $\tilde{\boldsymbol{\Theta}}$ is an approximation that converges to the TB bond-order or density matrix with increasing order n_max of the expansion.

The force may be decomposed in pairwise contributions

$$\boldsymbol{F}_{ik} = -\nabla_k U_{\mathrm{B},i} = -\sum_{\alpha j\beta}^{i\alpha \neq j\beta} \tilde{\Theta}_{i\alpha j\beta} \nabla_k H_{i\alpha j\beta} - \nabla_k U_{\mathrm{rep},i} \,, \tag{133}$$

so that

$$\boldsymbol{F}_k = \sum_{i}^{i\neq k} \boldsymbol{F}_{ik} \,. \tag{134}$$

The pairwise forces are the basis for the analytic computation of the stress tensor [49].

In magnetic simulations, the expressions for the torques may be obtained from the derivative of the energy with respect to the spin direction $s_{i\alpha}$ associated to each orbital. This involves expressions that may also be based on equation (130) [8, 46].

6. Parameterization of BOPs

The parameters of the TB bond model have to be defined before actual simulations can be carried out. In the following we will briefly discuss these parameters and describe how they are defined in a simple *d*-valent model for refractory bcc elements. In principle, of course, all the parameters could be obtained by evaluating the relevant matrix elements from DFT [17, 18]. In practice often functions with a given form are fitted to the DFT matrix elements. These functions typically cannot represent all details of the DFT matrix elements but provide only approximate interpolations of the DFT data, which leads to a loss of accuracy and transferability of the resulting models. In the following we summarize a parameterization strategy for the bond-order potentials that was developed by Vitek and co-workers [50–52].

6.1. Fitting parameters

6.1.1. Parameters in the bond energy. For the evaluation of the bond energy the Hamiltonian matrix elements are required. Here we work with an orthogonal TB model for the BOPs, therefore we do not need a parameterization of the overlap matrix. We model the valence of the transition metal elements with *d*-orbitals only. This may be justified as the *s*-orbitals contribute little to directional bond formation and mainly to a volume dependent energy that we will combine with the repulsive energy, but one should be aware that *sd*-hybridization may have a significant effect on structural stability in transition metals [53].

The *d*-orbitals are localized on the atoms and have only little overlap with orbitals on neighbouring atoms. We neglect the small overlap of the *d*-orbitals, which means that the screening matrix in equation (68) vanishes $\mathfrak{V} = 0$ and we may represent the Hamiltonian matrix within the two-centre Slater–Koster approximation, so that it only depends on the pairwise distance R_{ij} between atoms i and j. For a *d*-valent element only the Hamiltonian matrix elements $\beta_{dd\sigma}(R_{ij})$, $\beta_{dd\pi}(R_{ij})$ and $\beta_{dd\delta}(R_{ij})$ are different from zero, equation (55). Here we choose to parameterize these three distance-dependent functions using the so-called GSP function [54]. The GSP function is given by

$$\beta(R) = \beta(R_0)\left(\frac{R_0}{R}\right)^{n_a} \exp\left\{n_b\left[\left(\frac{R_0}{R_c}\right)^{n_c} - \left(\frac{R}{R_c}\right)^{n_c}\right]\right\}. \tag{135}$$

where R_0 is the first nearest-neighbour distance in the bcc ground state. The GSP function reintroduces the screening of second-neighbour bonds that we explicitly neglected by assuming $\mathfrak{V} = 0$ so that the Hamiltonian matrix for second and further neighbours may decline faster than a power law or simple exponential. For each of the three functions $\beta_{dd\sigma}$, $\beta_{dd\pi}$ and $\beta_{dd\delta}$ five parameters need to be set: $\beta(R_0)$, n_a, n_b, n_c and R_c.

For the onsite matrix elements $E_{i\alpha} = H_{i\alpha i\alpha}$ we also neglect any environmental dependence in equation (84) and just take them as constant. We furthermore assume that the onsite levels for all five of the *d*-orbitals are identical. As for the present example we are only interested in the parameterization of a BOP for a single element and not a binary or ternary material and

each of the atoms has only d-orbitals with identical onsite levels, all the reference onsite levels are identical and we choose to set them to zero

$$E_{i\alpha}^{(0)} = E_{i\alpha}^{(\mathrm{at})} = 0\,. \tag{136}$$

This completes the definition of all parameters in the bond energy.

6.1.2. Parameters in the promotion energy. As in our simple model all onsite levels of an atom are identical, it is not possible to promote an electron within an atom and the promotion energy vanishes identically,

$$U_{\mathrm{prom}} = 0\,. \tag{137}$$

This would of course be different for a model for a sp-valent element, such as silicon or carbon, where the promotion of electrons from the s state to the p states within the same atom is essential for describing sp, sp^2 or sp^3 hybridization and the resulting angular dependence of bond formation.

6.1.3. Parameters associated with charge transfer. For the simulation of close-packed metals one may assume that charge transfer between the atoms is small and may be neglected. Therefore in the following we further simplify our model by assuming local charge-neutrality, which implies that

$$q_i = 0\,. \tag{138}$$

This means that the contributions associated with charge transfer in equation (103) vanish identically,

$$U_{\mathrm{ion}} = U_{\mathrm{es}} = 0\,. \tag{139}$$

6.1.4. Parameters in the repulsive energy. While the second-order expansion of DFT defines the repulsive energy equation (96) unambiguously, it is common practice to parameterize the repulsive energy *ad-hoc*. For the BOP parameterization that we discuss here, the repulsive energy is written as

$$U_{\mathrm{rep}} = U_{\mathrm{pair}} + U_{\mathrm{env}} + U_{\mathrm{core}}\,, \tag{140}$$

and contains a pairwise term U_{pair} that mimics the overlap repulsion and also integrates approximately the volume dependent contribution of the s-electrons and a second pairwise term U_{core} for modelling the repulsion at short-distances. Furthermore, the non-pairwise character of the repulsive energy together with contributions from the s-electrons is approximated by an environmentally-dependent contribution U_{env}.

The pair contribution U_{pair} is represented by a cubic spline based on nodes at radii R_k with coefficients A_k,

$$U_{\mathrm{pair}} = \frac{1}{2}\sum_{ij}^{i\neq j}\sum_{k=1}^{4} A_k(R_k - R_{ij})^3, \tag{141}$$

for $R_k > R_{ij}$ and vanishes between the second and third nearest neighbour in the bcc structure. We use a power-law for the short-range repulsion

$$U_{\text{core}} = A\frac{(R_c - R_{ij})^k}{R_{ij}^l}, \tag{142}$$

which is different from zero only at distances shorter than the first-nearest neighbour of the bcc ground state. The non-pairwise contributions to the repulsion are modelled by a Yukawa-type function [55]

$$U_{\text{env}} = \frac{1}{2}\sum_{ij}^{i\neq j} V(r_{ij})\mathrm{e}^{-\frac{1}{2}(\lambda_i+\lambda_j)(r_{ij}-2r_{\text{core}})}, \tag{143}$$

where

$$V(r_{ij}) = \frac{A}{r_{ij}} \quad \text{and} \quad \lambda_i = \lambda_0 + \left[\sum_{k\neq i} B\mathrm{e}^{-\nu r_{ik}}\right]^{1/m}. \tag{144}$$

Recently, an alternative functional form for U_{env} was employed by Lin and co-workers [56] for BOP parameterizations of bcc transition metals,

$$U_{\text{env}} = \frac{1}{2}\sum_{ij}^{i\neq j} V(r_{ij})\mathrm{e}^{-(\lambda_i+\lambda_j)(r_{ij}-r_{\text{S}})} \tag{145}$$

where

$$V(r_{ij}) = A\mathrm{e}^{-\mu r_{ij}} \quad \text{and} \quad \lambda_i = \sum_{k\neq i} B\mathrm{e}^{-\nu r_{ik}}. \tag{146}$$

This alternative functional form is motivated by non-orthogonal TB calculations for the overlap of s and p closed-shell electrons in solid Ar [57].

6.2. Fitting procedure

The parameters in the bond energy and the repulsive energy need to be set before a BOP simulation may be carried out. Although a number of simplifications were made on the functional form of the bond and repulsive energy in the previous section, their dependence on the parameters is still non-linear and the determination of the best values for the parameters is not a straightforward task.

The parameters are typically determined by varying them until the mean square difference between reference data from DFT or experiment and the BOP prediction is minimized. The reference data typically comprises cohesive energies, lattice constants, elastic constants, defect energies, etc. Most of the difficulties in the parameterization of potentials arise from the limited transferability of the potential. A direct consequence of this limited transferability is that the optimum value of the parameters will be dependent on the reference data that is used in the fit. If the reference data contains only similar atomic environments, then we may expect that a potential may reproduce the reference data with good accuracy while at the same time the transferability to atomic environments not contained in the fit may be limited. If, on the other hand, the reference data contains very different atomic environments, then we expect that a potential with limited transferability will not be able to fit the reference data very well. In this way the best fit of a potential is not well defined but rather a matter of choice and taste of the person who parameterized the potential by balancing the limited transferability with the reference data and target application.

By introducing fitting protocols in which the parameters of the potential are determined in a well defined sequence, much of the ambiguity may be removed from the fitting procedure. In the following we illustrate a fitting protocol that was introduced by Vitek and coworkers for the fitting of the BOPs [50–52].

The fitting protocol contains the following steps:

(a) Obtain the parameters for the bond integrals in GSP form, equation (135). The GSP functions are fitted to bond integrals obtained by projection of the DFT wavefunctions on a minimal basis. In the work of Vitek and others [50–52] the bond integrals as well as the number of d-electrons per atom were obtained from TB-LMTO [58] calculations.
(b) Fit the environmentally-dependent contribution to U_{rep}, equation (143), to reproduce the Cauchy pressure for the ground state structure [59]. For the bcc elements that we consider here, the Cauchy pressure is given by the elastic constants as $C_{12} - C_{44}$.
(c) Fit the pair potential equation (141) to reproduce the cohesive energy E_{coh}, the lattice parameter a_0, as well as the remaining elastic constants C_{11} and $C_{12} + C_{44}$ for the bcc ground state structure.

This protocol uses only data for the ground state structure of the bcc elements in the fit. In the parameterization of the BOPs that we will discuss in the following, the short-ranged repulsion equation (142) and slight variations of the number of d-electrons were also fitted to reproduce interstitial point defects [60]. The BOP expansion used nine moments $n_{\max} = 9$, similar to previous work [50, 51].

6.3. Validation of the parameterization

In the following we discuss the quality of the parameterization by comparing to reference data that was not used for the fitting of the potential. We evaluate the transferability of the potential from the prediction of the energy of crystal structures, point defects and grain boundaries.

6.3.1. Structural energy differences. A critical test of the transferability of the BOP parameterization is the relative structural stability of different crystal structures. Figure 7 (left) shows the energy of crystal structures using the parametrization for Nb [60] as compared to DFT reference calculations. The BOP predicts the energy of the A15, fcc and sc crystal structures with good accuracy even though the parameterization was obtained only from properties of the bcc ground state structure. An additional test of the energy along the Bain path that transforms the bcc structure ($c/a = 1$) into the fcc structure ($c/a = \sqrt{2}$) is shown in figure 7 (right). The BOP predictions reproduce the DFT reference in good quantitative agreement. A similar transferability is achieved for the trigonal, hexagonal and orthorhombic transformations paths, also for BOP parameterizations for W, Mo and Ta [60]. The previous BOP parameterizations for Mo [50] and W [51] that used the same fitting protocol showed similar transferability to different crystal structures and structural transformation paths.

6.3.2. Vacancies and interstitials. Point defects represent a significant distortion of the electronic structure of a homogeneous crystal phase. Therefore the prediction of point defect energies is a difficult challenge for a potential for which only properties of the bcc ground state phase were taken into account in the parameterization. At the same time the formation and activation energy of point defects are key parameters that determine the diffusion and therefore the kinetics of transformations in the solid state and it is therefore important that a potential provides a sensible description of point defects.

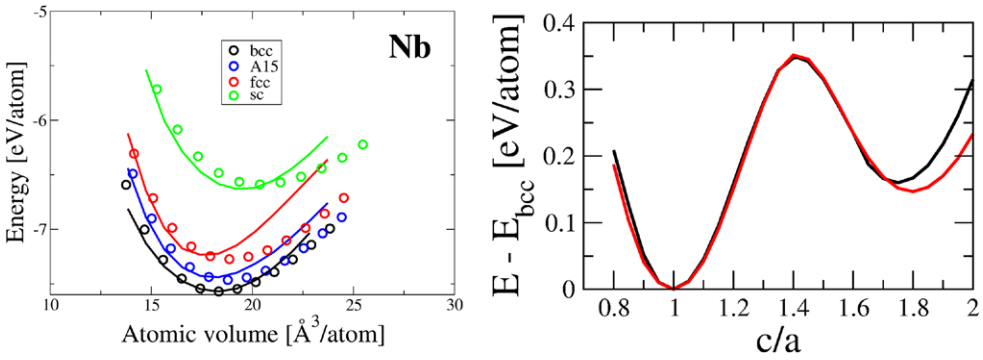

Figure 7. Structural energy differences (left, lines: BOP, symbols: DFT) and binding energy along tetragonal transformation path (black line: BOP, red line: DFT) for Nb. Taken from [60].

Using the fitting protocol outlined above, a good match of the formation energies of single vacancies and different types of interstitials in bcc refractory elements can be achieved [60]. By choosing the *d*-electron number slightly different from the DFT reference, the correct energetic ordering of different self-interstitial point defects could be obtained, see figure 8 (left). The energy barrier for vacancy diffusion, see figure 8 (right), also shows a sensible agreement with DFT calculations [61] for the Ta and Mo BOP parameterizations [60]. For Nb and W the BOP parameterization significantly overestimates the energy barrier. These findings suggest that the present fitting protocol does not guarantee that migration barriers are reproduced quantitatively. This is not unexpected as at the migration barrier the diffusing atoms are very close to their neighbours and these short interatomic distances and large local distortions were not sampled by the reference data.

6.3.3. Grain boundaries. In addition to point defects, extended defects such as line defects (dislocations) and planar defects (interfaces and surfaces) are a good probe for testing the transferability of a potential as they are also associated with large changes in the electronic structure and bond formation. Here we discuss results for planar defects, specifically the $\Sigma5(3\,1\,0)[0\,0\,1]$ symmetric tilt grain boundary (STGB). This STGB is of particular interest as for some of the bcc transition metals the mirror symmetry is not preserved in the minimum-energy structure, instead one finds a relative displacement of the two grains. DFT calculations [62] found the most stable grain boundary structure for a displacement along $[1\,0\,0]$ for Mo and W. For Ta the mirror symmetry of the grain boundary is preserved, for Nb the energy difference is at the limit of DFT accuracy. A subsequent study for Nb and Mo showed that TB/BOP describe the macroscopic shift correctly in contrast to second-moment approximations [63]. We carried out similar calculations using parameterizations for W, Mo, Ta and Nb [60]. We show the results for Mo in figure 9. The displacement along the $[0\,0\,1]$ direction lowers the grain-boundary formation energy, see left-hand panel of figure 9. The numerical value $0.06a_0$ is too small compared to the DFT reference of $0.20a_0$. The perpendicular displacement, the change of the distance between the two grains in the $[3\,1\,0]$ direction by $0.06a_0$ is in excellent agreement with the DFT result (also $0.06a_0$), see right-hand panel of figure 9. The BOPs furthermore confirm the DFT prediction that the mirror symmetry is broken for W while it is preserved for Ta. For Nb the BOP predicts a broken mirror symmetry. These calculations demonstrate that BOPs that were parameterized based on the bcc bulk structure

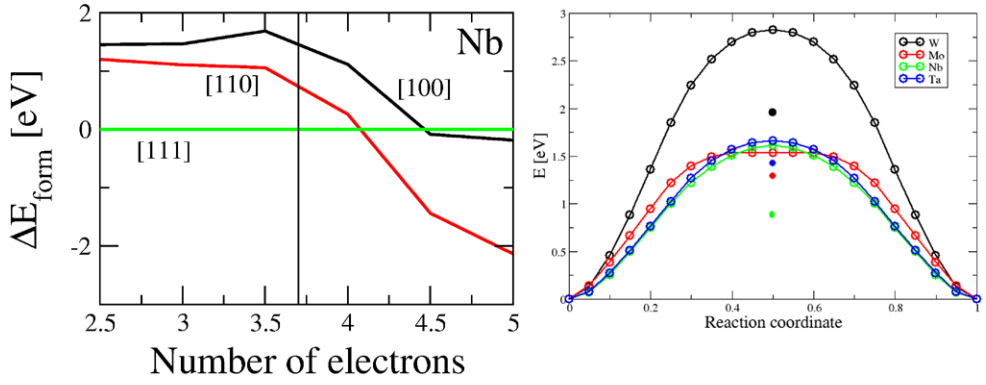

Figure 8. (Left) Influence of *d*-electron count on energetic ordering of the [1 0 0], [1 1 0] and [1 1 1] self-interstitial defects in Nb. (Right) Energy barrier for vacancy diffusion in W, Ta, Nb and Mo. The lines correspond to BOP predictions, the single data points at 0.5 were obtained by DFT calculations [61].

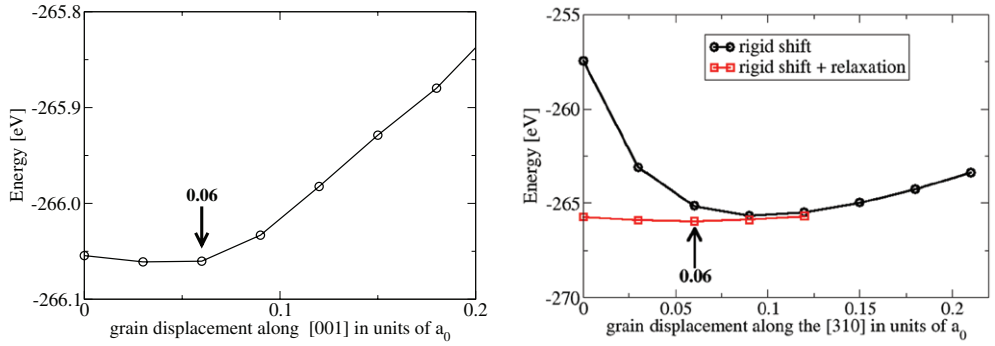

Figure 9. Translation of Σ5(3 1 0)[0 0 1] symmetric tilt grain boundary along [0 0 1] (left) and [3 1 0] (right) in Mo as obtained by analytic BOP.

are transferable to grain boundaries. The limits of the parameterization become apparent at surfaces, i.e. an atomic environment with broken bonds. We find that the W BOP reproduces the correct ordering of surface energies with $\gamma(1\,0\,0) < \gamma(1\,1\,1) < \gamma(2\,1\,1) < \gamma(1\,1\,0)$, however, with a nearly constant shift of the order of 1 J m^{-2} to lower energies as compared to DFT results. This suggests that the overall change in the electronic structure at the surface is qualitatively captured by the BOPs but that the fit and possibly the underlying TB model needs to be refined for surface calculations.

6.4. BOP parameterizations for other materials

A large number of parameterizations for BOPs exists, e.g. for the transition metals Ti [64], Ti–Al [52], Mo [50], Ir [53], W [51], Fe [65], Mn [66] and bcc refractory metals [56, 60]. Only some of these parameterizations were obtained using the fitting protocol discussed here. A summary of parameterizations for different materials until 2009 is given in [67]. While there are many more parameterizations for orthogonal TB bond models, e.g. for Ti–C/N [18, 68,

69], Fe [17], Fe–Cr–Mn [70], Fe–C [71, 72] and Co/Ni clusters [25], to give just a few selected examples, only some of these parameterizations were directly adopted in BOP calculations.

7. Conclusion

The BOPs are derived from DFT at two levels of coarse graining. The second-order expansion of the DFT energy is cast in the TB bond model that contains covalent bond formation as well as charge transfer and magnetism and therefore is applicable to modelling a large class of materials. The BOP expansion achieves a good approximation to the TB energies at a moderate number of moments such that linear-scaling simulations with millions of atoms are possible.

While in principle the BOPs could be parameterized directly by evaluating DFT matrix elements, in practice additional approximations and simplifications are introduced. In particular, the functional form of the repulsion is only partly justified from DFT. By parameterising the BOPs along a well-defined fitting protocol, the dependence of the parameterization on the reference data is partly removed.

Although the fitting protocol only uses information from the ground state structure, the BOPs are transferable to other crystal phases and predict point defects and interfaces in good agreement with DFT reference calculations. This may be attributed to the derived functional form of the BOPs. The representation of the interatomic interaction in the TB bond model is general and flexible and therefore transferable between very different atomic environments, in contrast to empirical potentials. Because the TB bond model is obtained from DFT, its predictions are in good agreement with DFT even far away from atomic environments that were used as reference data in the construction of the BOPs.

The parameterization of the BOPs presented here is limited mainly by the neglect of environmental dependence in the bond integrals and an *ad-hoc* formulation of the repulsive energy. By taking into account the environmental dependence of the bond integrals and a more careful derivation of the repulsive energy, together with an extension of the fitting protocol to include a wider variety of atomic environments, we expect that the transferability of the next generation of BOP parameterizations will be significantly improved.

Acknowledgments

We acknowledge fruitful discussion with S Schreiber and A Ladines. TH and RD acknowledge financial support through the DFG through projects C1 and C2 of the collaborative research center SFB/TR 103.

References

[1] Daw M S and Baskes M I 1984 *Phys. Rev.* B **29** 6443
[2] Finnis M W and Sinclair J E 1984 *Phil. Mag.* A **50** 45
[3] Tersoff J 1986 *Phys. Rev. Lett.* **56** 632
[4] Bartók A P, Payne M C, Kondor R and Csányi G 2010 *Phys. Rev. Lett.* **104** 136403
[5] Thompson A P, Swiler L P, Trott C M, Foiles S J and Tucker G 2015 *J. Comput. Phys.* **285** 316–30
[6] Behler J and Parrinello M 2007 *Phys. Rev. Lett.* **98** 146401
[7] Sutton A P, Finnis M W, Pettifor D G and Ohta Y 1988 *J. Phys.* C **21** 35
[8] Drautz R and Pettifor D G 2011 *Phys. Rev.* B **84** 214114
[9] Foulkes W M C and Haydock R 1989 *Phys. Rev.* B **39** 12520

[10] Elstner M, Porezag D, Jungnickel G, Elsner J, Haugk M, Frauenheim T, Suhai S and Seifert G 1998 *Phys. Rev.* B **58** 7260
[11] Finnis M W 2007 *Interatomic Forces in Condensed Matter* (Oxford: Oxford University Press)
[12] Pettifor D G 1995 *Bonding and Structure of Molecules and Solids* (Oxford: Oxford University Press)
[13] Paxton A T 2009 Institute for Advanced Simulation, Forschungszentrum Jülich *Multiscale Simulation Methods in Molecular Sciences* (*NIC Series* vol 42) (ed) J Grotendorst *et al* (Germany: Jülich Supercomputing Centre) p 145
[14] Pickett W E 1996 *J. Korean Phys. Soc.* **29** S70
[15] Paxton A T and Finnis M W 2008 *Phys. Rev.* B **77** 024428
[16] Löwdin P O 1950 *J. Chem. Phys.* **18** 365
[17] Madsen G K H, McEniry E J and Drautz R 2011 *Phys. Rev.* B **83** 184119
[18] Urban A, Reese M, Mrovec M, Elsässer C and Meyer B 2011 *Phys. Rev.* B **84** 155119
[19] Pettifor D G and Oleinik I I 1999 *Phys. Rev.* B **59** 8487
[20] Pettifor D G and Oleinik I I 2000 *Phys. Rev. Lett.* **84** 4124
[21] Drautz R, Murdick D A, Nguyen-Manh D, Zhou X W, Wadley H N G and Pettifor D G 2005 *Phys. Rev.* B **72** 144105
[22] Alinaghian P, Gumbsch P, Skinner A J and Pettifor D G 1993 *J. Phys.: Condens. Matter* **5** 5795
[23] Slater J C and Koster G F 1954 *Phys. Rev.* **94** 1498
[24] Drautz R, Zhou X W, Murdick D A, Gillespie B, Wadley H N G and Pettifor D G 2007 *Prog. Mater. Sci.* **52** 196
[25] McEniry E J, Drautz R and Madsen G K H 2013 *J. Phys.: Condens. Matter* **25** 115502
[26] Margine E R and Pettifor D G 2014 *Phys. Rev.* B **89** 235134
[27] Nguyen-Manh D, Pettifor D G and Vitek V 2000 *Phys. Rev. Lett.* **85** 4136
[28] Sheppard T J, Lozovoi A Y, Pashov D L, Kohanoff J J and Paxton A T 2014 *J. Chem. Phys.* **141** 044503
[29] Lozovoi A Y, Sheppard T J, Pashov D L, Kohanoff J J and Paxton A T 2014 *J. Chem. Phys.* **141** 044504
[30] Lozovoi A Y, Pashov D L, Sheppard T J, Kohanoff J J and Paxton A T 2014 *J. Chem. Phys.* **141** 044505
[31] Hubbard J 1963 *Proc. R. Soc.* A **276** 238
[32] Pettifor D G 1989 *Phys. Rev.* B **63** 2480
[33] Drautz R and Pettifor D G 2006 *Phys. Rev.* B **74** 174117
[34] Horsfield A P, Bratkovsky A M, Fearn M, Pettifor D G and Aoki M 1996 *Phys. Rev.* B **53** 12694
[35] Horsfield A P, Bratkovsky A M, Pettifor D G and Aoki M 1996 *Phys. Rev.* B **53** 1656
[36] Hammerschmidt T and Drautz R 2009 *Multiscale Simulation Methods in Molecular Science* (*NIC Series* vol 42) (ed) J Grotendorst *et al* (Jülich: Jülich Supercomputing Centre) p 229
[37] Čák M, Hammerschmidt T and Drautz R 2013 *J. Phys.: Condens. Matter* **26** 265002
[38] Haydock R 1980 *Solid State Phys.* **35** 215
[39] Seiser B, Pettifor D G and Drautz R 2013 *Phys. Rev.* B **87** 094105
[40] Silver R N and Röder H 1994 *Int. J. Mod. Phys.* C **5** 735
[41] Silver R N, Röder H, Voter A F and Kress J D 1996 *J. Comput. Phys.* **124** 115
[42] Voter A F, Kress J D and Silver R N 1996 *Phys. Rev.* B **53** 12733
[43] Goedecker S and Colombo L 1994 *Phys. Rev. Lett.* **73** 122
[44] Goedecker S and Teter M 1995 *Phys. Rev.* B **51** 9455
[45] Ford M E, Drautz R, Hammerschmidt T and Pettifor D G 2014 *Mod. Simul. Mater. Sci. Eng.* **22** 034005
[46] Ford M, Pettifor D G and Drautz R 2015 *J. Phys.: Condens. Matter* **27** 086002
[47] Hellmann H 1937 *Einführung in die Quantenchemie* (Leipzig: Deuticke)
[48] Feynman R P 1939 *Phys. Rev.* **56** 340
[49] Schreiber S, Čák M, Hammerschmidt T and Drautz R 2015 in preparation
[50] Mrovec M, Nguyen-Manh D, Pettifor D G and Vitek V 2004 *Phys. Rev.* B **69** 094115
[51] Mrovec M, Gröger R, Bailey A G, Nguyen-Manh D, Elsässer C and Vitek V 2007 *Phys. Rev.* B **75** 104119
[52] Znam S, Nguyen-Manh D, Pettifor D G and Vitek V 2003 *Phil. Mag.* **83** 415
[53] Cawkwell M J, Nguyen-Manh D, Pettifor D G and Vitek V 2006 *Phys. Rev.* B **73** 064104
[54] Goodwin L, Skinner A J and Pettifor D G 1989 *Europhys. Lett.* **9** 701
[55] Nguyen-Manh D, Pettifor D G, Cockayne D J H, Mrovec M, Znam S and Vitek V 2003 *Bull. Mater. Sci.* **26** 43

[56] Lin Y S, Mrovec M and Vitek V 2014 *Mod. Simul. Mater. Sci. Eng.* **22** 034002
[57] Aoki M and Kurokawa T 2007 *J. Phys.: Condens. Matter* **19** 236228
[58] Nguyen-Manh D, Vitek V and Horsfield A 2007 *Prog. Mater. Sci.* **52** 255
[59] Šob M and Vitek V 1996 *Stability of Materials* (*NATO Advanced Science Institute, Series B: Physics* vol 355) (ed) A Gonis *et al* (New York: Plenum) p 449
[60] Čák M, Hammerschmidt T, Rogal J, Vitek V and Drautz R 2014 *J. Phys.: Condens. Matter* **26** 195501
[61] Nguyen-Manh D, Horsfield A P and Dudarev S L 2006 *Phys. Rev.* B **73** 020101
[62] Ochs T, Beck O, Elsässer C and Meyer B 2000 *Phil. Mag.* A **80** 351
[63] Ochs T, Elsässer C, Mrovec M, Vitek V, Belak J and Moriarty J 2000 *Phil. Mag.* A **80** 2405
[64] Girshick A, Bratkovsky A M, Pettifor D G and Vitek V 1998 *Phil. Mag.* A **77** 981
[65] Mrovec M, Nguyen-Manh D, Elsässer C and Gumbsch P 2011 *Phys. Rev. Lett.* **106** 246402
[66] Drain J F, Drautz R and Pettifor D G 2014 *Phys. Rev.* B **89** 134102
[67] Hammerschmidt T, Drautz R and Pettifor D G 2009 *Int. J. Mater. Res.* **100** 11
[68] Margine E R, Kolmogorov A N, Reese M, Mrovec M, Elsässer C, Meyer B, Drautz R and Pettifor D G 2011 *Phys. Rev.* B **84** 155120
[69] Gehrmann J, Pettifor D G, Kolmogorov A N, Reese M, Mrovec M, Elsässer C and Drautz R 2015 *Phys. Rev.* B **91** 054109
[70] McEniry E, Madsen G K H and Drautz R 2011 *J. Phys.: Condens. Matter* **23** 276004
[71] Hatcher N, Madsen G K H and Drautz R 2012 *Phys. Rev.* B **86** 155115
[72] Paxton A T and Elsässer C 2013 *Phys. Rev.* B **87** 224110